# Iron nanoparticles derived from rooibos tea extract supported polymer for $Cr^{6+}$ removal


**S.M Matome**

**orcid.org 0000-0003-1923-2357**


**Dissertation submitted in fulfilment of the requirements for the degree *Master of Science in Chemistry* at the North-West University**

**Supervisor: Prof L.M Katata-Seru**
**Co-supervisors: Prof A Maity**
**Prof M.J Hato**

**Graduation ceremony April 2019**
**Student number: 23886064**

## DECLARATION

I Sarah Makgamathwane Matome herewith declare that the dissertation entitled, "*Iron nanoparticles derived from rooibos tea extract supported polymer for* $Cr^{6+}$ *removal*", which I herewith submit to the North-West University as completion of the requirements set for the Master's degree, is my own work and has not already been submitted to any other university. I understand and accept that the copies that are submitted for examination are the property of the University.

Signature of candidate_____

University number_____

Signed at _____ this _____day of _____ 20__.

## ABSTRACT

Deterioration of water quality due to the presence of toxic heavy metals in environmental water resources introduced by industrial pollution is a serious matter of concern today. Only around 20% of the global wastewater was properly treated until 2015. Furthermore, in developing countries, approximately 70% of the industrial wastewater is not properly discharged. Chromium is a common heavy metal contaminant with two major species that is the, trivalent Cr(III) and hexavalent Cr(VI). Due to its higher solubility and mobility in environments, Cr(VI) is highly toxic and carcinogenic while Cr(III) is an essential micronutrient in trace amount for mammals.

Therefore, the objective of the study was to synthesize low-cost $Fe^0$ nanoparticles (NPs) supported in polypyrrole (Ppy) to investigate their effectiveness in Cr(VI) removal from aqueous solutions. Moreover, the effect of temperature, contact time, pH, adsorbent dose, and effect of co-existing ions were assessed. Ppy/$Fe^0$ nanocomposite (NC) was characterized using various techniques such as attenuated total reflectance-Fourier transform infrared spectroscopy (ATR-FTIR), field emission-scanning electron microscopy (FE-SEM), high resolution-transmission electron microscopy (HR-TEM), Braunner-Emmet-Teller (BET) and X-ray diffractometry (XRD).

An increase in Cr(VI) removal due to pH was observed when pH was increased, the removal decreased from 73 - 32% and the optimum was at pH 2.0. The kinetic adsorption data fitted the pseudo-second-order model. The adsorption isotherm followed the Langmuir isotherm model with the maximum sorption capacity of 305.8 $mg.g^{-1}$ at 25℃ and the adsorption process was endothermic. The specific surface area of the synthesized nanocomposite was calculated to be 80.53 $m^2.g^{-1}$ by the BET method. TEM images clearly showed the core/shell structure of the Ppy/$Fe^0$ NC. Based on the findings from the study, it is hypothesized that results obtained may assist the wastewater treatment field with easy and safe removal of heavy metals from water.



Keywords: Adsorption; nanocomposite; removal; wastewater; hexavalent chromium

## ACKNOWLEDGEMENTS

I would like to wholeheartedly express my gratitude to everyone who contributed towards the success of this research. It would not have been possible without your input, time, encouragement and support. Without you, nothing would have been possible. Now I understand the African proverb “It takes a village to raise a child”.

- First and foremost I would like to thank The Almighty Lord for the love, everlasting mercy and the strength He provided me with which translated to the completion of this study.
- My supervisors: Prof Katata-Seru, Prof Arjun Maity and Prof Mpitloane Hato for their encouragement and determination to see me succeed. No words can ever express my gratitude to them.
- My lab mates: for their encouragement and support.
- CSIR (NCNSM): for the warm welcome and assistance.
- My family and friends: for their continued support, love and believing in me. You have been the wind beneath my wings.
- Lastly, I would like to sincerely thank North-West University and NRF/SASOL for the financial support.

## DEDICATION

My lovely daughter Onalenna Matome, you have been my source of strength and have brought meaning to my life. My mother Meriam Matome, the one who always believed in me. You would give your all to see me succeed. My late father Moses Matome, my guardian angel always looking down on me from heaven.

## RESEARCH CONTRIBUTIONS

Sarah Matome, Lebogang Katata-Seru, Arjun Maity, Mpitloane Hato, Green synthesis of $Fe^0$ nanoparticles encapsulated in polypyrrole for toxic Cr(VI) removal, Andrew Crouch Honorary Symposium, 21 July 2018, Cape Town, South Africa (Oral presentation).

Sarah Matome, Lebogang Katata-Seru, Arjun Maity, Mpitloane Hato, Removal of toxic Cr(VI) by Ppy/$Fe^0$ nanocomposite, Sustainable Sanitation Waste and Water Management Conference, 20 – 23 November 2018, Cape Town, South Africa (Accepted for oral presentation).

Sarah Matome, Lebogang Katata-Seru, Arjun Maity, Mpitloane Hato, $Fe^0$ nanoparticles supported in polypyrrole for toxic Cr(VI) removal, 43rd National Convention of the South African Chemical Institute, 02 – 07 December 2018, Pretoria, South Africa (Accepted for poster presentation).

Sarah Matome, Arjun Maity, Lebogang Katata-Seru, Mpitloane Hato ,Green synthesis of $Fe^0$ nanoparticles using rooibos tea extract encapsulated in polypyrrole for toxic Cr(VI) removal (will be submitted to *Journal of Molecular Liquids)*.

## TABLE OF CONTENT

DECLARATION ..... i
ABSTRACT ..... ii
ACKNOWLEDGEMENTS ..... iii
DEDICATION ..... iv
RESEARCH CONTRIBUTIONS ..... v
TABLE OF CONTENT ..... vi
LIST OF ABBREVIATIONS ..... ix
LIST OF FIGURES ..... x
CHAPTER 1 ..... 1
INTRODUCTION ..... 1
1.1 General introduction ..... 1
1.2 Problem statement ..... 3
1.3 Research aim and objectives ..... 3
1.4 Outline of the dissertation ..... 4
REFERENCES ..... 5
CHAPTER 2 ..... 7
LITERATURE REVIEW ..... 7
2.1 Water treatment using nanotechnology ..... 7
2.2 Green synthesis ..... 9
2.3 Chemistry of Chromium ..... 11
2.4 Chromium species ..... 11
2.5 Application and toxicity of chromium ..... 12
2.6 Overview of *Asphalathus linearis* ..... 13
2.7 Choice of polymer ..... 15
2.8 Adsorption as an efficient method for removing pollutants ..... 16
2.9 Adsorption isotherm models ..... 19

2.9.1 Langmuir isotherm model ..... 19
2.9.2 Freundlich isotherm model ..... 20
2.10 Kinetic models ..... 20
2.10.1 Pseudo-first order ..... 20
2.10.2 Pseudo-second order ..... 21
2.11 Current research approach ..... 21
2.12 Concluding remarks ..... 22
REFERENCES ..... 23
CHAPTER 3 ..... 30
METHODOLOGY ..... 30
3.1 Materials ..... 30
3.2 Experimental methods ..... 30
3.2.1 Preparation of Rooibos extract ..... 30
3.2.2 Synthesis of $Fe^0$ NPs using rooibos extract ..... 30
3.2.3 Synthesis of adsorbent ..... 31
3.3 Characterization instruments ..... 31
3.3.1 Ultraviolet-visible (UV-vis) spectroscopy ..... 31
3.3.2 Attenuated total reflectance-Fourier transform infrared (ATR-FTIR) spectroscopy ..... 31
3.3.3 X-ray diffraction (XRD) spectroscopy ..... 31
3.3.4 Field emission-scanning electron microscopy (FE-SEM) ..... 32
3.3.5 High resolution-transmission electron microscopy (HR-TEM) ..... 32
3.3.6 Malvern zetasizer ..... 33
3.3.7 Brauner-Emmett-Teller (BET) surface area analysis ..... 32
3.5 Batch adsorption experiments ..... 33
3.5.1 Effect of different compositions of the Ppy/$Fe^0$ NC ..... 35
3.5.2 Effect of pH ..... 34
3.5.3 Effect of contact time ..... 34

3.5.4 Effect of temperature ..... 34
3.5.5 Effect of adsorbent dose ..... 35
3.5.6 Adsorbent regeneration studies ..... 35
3.5.7 Effect of co-existing ions ..... 35
REFERENCES ..... 36
CHAPTER 4 ..... 37
RESULTS AND DISCUSSION ..... 37
SECTION 1: Characterization of $Fe^0$ NPs, Ppy and Ppy/$Fe^0$ NC ..... 37
4.1 ATR-FTIR ..... 37
4.2 X-ray diffraction ..... 38
4.3 SEM analysis ..... 39
4.5 TEM analysis ..... 41
4.6 Particle size of $Fe^0$ NPs ..... 44
4.7 BET ..... 43
SECTION 2: Evaluation of the Ppy/$Fe^0$ NC on Cr(VI) adsorption ..... 44
4.8 Effect of pH ..... 44
4.9 Effect of adsorbent dose ..... 45
4.10 Adsorption isotherm ..... 46
4.11 Adsorption kinetics ..... 51
4.12 Adsorbent regeneration studies ..... 56
4.13 Effect of co-existing ions ..... 57
REFERENCES ..... 59
CHAPTER 5 ..... 62
CONCLUSION AND RECOMMENDATIONS ..... 62
5.1 Conclusion ..... 62
5.2 Recommendations ..... 63

## LIST OF ABBREVIATIONS

| | | |
|---|---|---|
| **ATR-FTIR** | **:** | Attenuated total reflectance-Fourier transform infrared spectroscopy |
| **BET** | **:** | Braunner-Emmett-Teller |
| **Cr(III)** | | Trivalent chromium |
| **Cr(VI)** | **:** | Hexavalent chromium |
| **EC** | **:** | Electrical conductivity |
| **EDX** | **:** | Energy-dispersive X-ray spectroscopy |
| **EPA** | **:** | Environmental Protection Agency |
| **$Fe^0$ NPs** | **:** | Zero-valent iron nanoparticles |
| **FE-SEM** | **:** | Field emission-scanning electron microscopy |
| **HR-TEM** | **:** | High resolution-transmission electron microscopy |
| **NC** | **:** | Nanocomposite |
| **NMs** | **:** | Nanomaterials |
| **NPs** | **:** | Nanoparticles |
| **Ppy** | **:** | Polypyrrole |
| **Py** | **:** | Pyrrole |
| **U.S EPA** | **:** | United States Environmental Protection Agency |
| **UNICEF** | **:** | United Nations Children's Fund |
| **UV-vis** | **:** | Ultraviolet-visible spectroscopy |
| **WHO** | **:** | World Health Organization |
| **XRD** | **:** | X-ray diffraction |

## LIST OF FIGURES

**Figure 2.1:**Synthesis of metallic NPs using plant extracts ..... 10
**Figure 2.2:**Cr(VI) species distribution at different pH. ..... 12
**Figure 2.3:**(a) Rooibos plant, (b) fermented rooibos leaves and (c) unfermented rooibos leaves. ..... 13
**Figure 2.4:** Some of the major bioactive molecular compounds within the rooibos extract. ..... 14
**Figure 2.5:**A probable mechanism for the removal of Cr(VI) ions from aqueous solution. ..... 15
**Figure 2.6:**Protonation/deprotonation technique of Ppy. ..... 16
**Figure 2.7:** Some of the methods for pollutant removal. ..... 17
**Figure 2.8:** Adsorption mechanism. ..... 18
**Figure 4. 1:** ATR-FTIR spectra of $Fe^0$ NPs, Ppy/$Fe^0$ NC before and after adsorption. ..... 38
**Figure 4. 2:**XRD patterns of Ppy/$Fe^0$ NC before and after adsorption. ..... 39
**Figure 4. 3:**SEM images of a) Ppy homopolymer and b) Ppy/$Fe^0$ NC. ..... 40
**Figure 4. 4:**EDX of Ppy/$Fe^0$ NC before and after Cr(VI) adsorption. ..... 41
**Figure 4. 5:**HR-TEM images of Ppy/$Fe^0$ NC. ..... 42
**Figure 4. 6:** Particle size distribution of $Fe^0$ NPs ..... 43
**Figure 4.7:** Effect of pH on Cr(VI) removal using Ppy/$Fe^0$ NC. ..... 44
**Figure 4.8:**Cr(VI) speciation in an aqueous environment as a function of Cr(VI) concentration and pH. ..... 45
**Figure 4.9:**Effect of adsorbent dose on Cr(VI) removal by Ppy/$Fe^0$ NC. ..... 46
**Figure 4.10:** Effect of temperature on Cr(VI) removal by Ppy/$Fe^0$ NC. ..... 47
**Figure 4.11:** Fit of data to linearized Langmuir isotherm model. ..... 48
**Figure 4.12:**Fit of data to linearized Freundlich isotherm model. ..... 48
**Figure 4.13:**Fit of data to Langmuir and Freundlich isotherm kinetic model. ..... 49
**Figure 4.14:**Effect of contact time on Cr(VI) removal by Ppy/$Fe^0$ NC. ..... 52
**Figure 4.15:** Fit of data to linearized pseudo-second order kinetic model. ..... 53
**Figure 4.16:** Fit of data to linearized pseudo-second order kinetic model. ..... 54
**Figure 4.17:**Fit of data to pseudo-first-order and pseudo-second-order kinetic models. ..... 54
**Figure 4.18:** Adsorption cycles for Cr(VI) removal by Ppy/$Fe^0$ NC. ..... 57

**Figure 4.19:** The effect of co-existing ions on Cr(VI) adsorption by Ppy/$Fe^0$ NC ..... 58

## LIST OF TABLES

**Table 2.1:** Examples of potential applications of nanotechnology in water/wastewater treatment. ..... 8
**Table 2.2:**Plant extracts used for nanoparticles synthesis ..... 10

**Table 4. 1:** Isotherm parameters for Cr(VI) adsorption by Ppy/$Fe^0$ NC ..... 50
**Table 4. 2 :**Comparison of the Cr(VI) adsorption capacity of Ppy/$Fe^0$ NC with other adsorbents ..... 51
**Table 4.3:**Kinetic parameters for Cr(VI) adsorption by Ppy/$Fe^0$ NC ..... 55

# CHAPTER 1

# INTRODUCTION

## 1.1 General introduction

One of the most important and basic natural resources is water [1]. Accessibility to clean and affordable water is a major challenge for the 21$^{st}$ century, and is considered one of the humanitarian goals [2]. It was estimated that 663 million people worldwide still used unimproved drinking water sources, including unprotected wells, springs and surface water in 2015 [3]. It is expected that the water supply will decrease by one-third in the coming years [4]. Groundwater has proven to be the most reliable source for meeting rural water demand in the Sub-Saharan Africa and supplies potable water to an estimated 1.5 billion people in the whole world. Nevertheless, groundwater resources are frequently vulnerable to pollution which lowers its quality [5].

Waste streams from the leather tannery, metal-plating, mining, and power generation operations contain toxic heavy metals such as chromium (Cr), lead (Pb), cadmium (Cd), and mercury (Hg) [6]. Cr has great economic importance in industrial use, however, it is one of the heavy metal pollutants and in the last few decades, the amount of Cr in water has increased as a result of human activities [7]. Drinking water supplies in many geographic areas contain Cr(III) and Cr(VI) [8]. Cr(VI) is directly active as a carcinogen and, once ingested, it can travel to a variety of organs by ingestion [9]. Human contact with Cr(VI) is known to cause adverse health problems like liver damage, vomiting, pulmonary congestion, severe skin irritation and ulceration [10]. Some reported removal methods for Cr(VI) include adsorption, reverse osmosis, electrochemical precipitation, bioadsorption, foam separation, separation by freezing and evaporation [11]. These methods are sometimes expensive and often inefficient at low concentrations [12]. Among the several emerging technologies, the development in nanotechnology has proven to be an incredible potential for wastewater remediation and different other environmental water treatment challenges [13].

Nanotechnology is among the most progressive innovations in the world and it depicts a scope of advancements performed on a nanometre scale with far reaching applications as an empowering technology in different industries [14]. It is the ability to manipulate, measure and manufacture things at an atomic or molecular scale, usually between 1-1000 nanometres [15]. Currently, advances in nanoscale science and engineering suggest that nanomaterials (NMs) have great potential to improve water quality in a cost-effective way and at the same time, increasing the reduction level of water contaminants [16].

Over the last decade, a great deal of research has focused on the removal of contaminants using the zero-valent iron nanoparticles ($Fe^0$ NPs) due to its non-toxicity, abundance, low cost, easy to produce, and also because its reduction process requires little maintenance. Due to the small particle size, large specific surface and high surface activity, $Fe^0$ NPs have been considered to be an effective material for the removal of heavy metals [17]. A direct application of $Fe^0$ NPs in water treatment system may cause iron pollution and loss of their particles due to their tiny particle size. $Fe^0$ NPs are easily agglomerated which restricts their field of application [18]. Hence, it is necessary to load $Fe^0$ NPs onto supporting materials for the treatment of pollutants [19]. The use of plants has proven to be an alternative to chemical and physical methods for the synthesis of NPs [20].

In this study rooibos extract was used to synthesize $Fe^0$ NPs supported on polypyrrole (Ppy), denoted Ppy/$Fe^0$ NC. Techniques such as attenuated total reflectance-Fourier transform Infrared spectroscopy (ATR-FTIR), field emission-scanning electron microscopy (FE-SEM), high resolution-transmission electron microscopy (HR-TEM), X-ray diffractometry (XRD) and Braunner-Emmet-Teller (BET) and were used to characterize the nanocomposite (NC). Ppy was chosen due to its good environmental stability, non-toxicity, good biocompatibility and low cost. The performance of the obtained NC was investigated for removal of Cr(VI) from water.

*Aspalathus linearis (A. linearis)* of the family Fabaceae, which is also known as rooibos, is a plant which originates in Southern Africa [21]. Rooibos has been used

for more than three centuries as a herbal tea by the local communities. Its phenolic composition gives it various health benefits such as antioxidant properties [22]. Spent rooibos biomass has been used as an adsorbent for dye removal [23].

## 1.2 Problem statement

The world is faced with threatening challenges in meeting rising demands of clean water as the accessible supplies of freshwater are being reduced due to population growth, extended droughts and competing demands from a variety of users [24]. Heavy metal pollution is the most significant environmental problem nowadays, and endangers the lives of human beings worldwide [25]. Traditional treatment processes like ion exchange, electrochemical and chemical precipitation can be used for removal of heavy metal from inorganic effluent [26]. Nevertheless, these methods have drawbacks such as high reagent and energy requirements, incomplete metal removal and generation of toxic sludge or other waste products that need careful disposal [27].

North West province is predominantly a dry area with very few rivers running annually. The province therefore depends on underground water for both its domestic and industrial water requirements [28]. Gold mining activities in the North West province have been linked with varying levels of heavy metal contamination that have posed potential risks to residents of surrounding informal settlements[29]. Hence, there is a need of using low-cost nanocomposite (NC) for heavy metal removal in wastewater treatment to overcome the disadvantages of the conventional methods previously used.

## 1.3 Research aim and objectives

The aim of the proposed study was to synthesize Ppy/$Fe^0$ NC for removal of Cr(VI) from aqueous solution.

The objectives of the study were to:

- Synthesize low-cost $Fe^0$ NPs through the green synthesis method using rooibos plant extract.
- Synthesize Ppy/$Fe^0$ NC by an *in-situ* chemical oxidative polymerization method.

- Characterize Ppy/$Fe^0$ NC using HR-TEM, FE-SEM, ATR-FTIR, BET, XRD and Malvern zetasizer.
- Carry out batch adsorption studies - effect of pH, adsorbent dose, co-existing ions, adsorption kinetics, and adsorption isotherm on Cr(VI) removal by Ppy/$Fe^0$ NC.

## 1.4 Outline of the dissertation

This dissertation consist of five chapters

**Chapter 1:** Gives a brief introduction of the study. It also highlights the global challenges concerning the quality of drinking water, and the aim and objectives of this study.

**Chapter 2:** Provides a detailed literature review of the study.

**Chapter 3:** Outlines all the materials used and the methodology followed.

**Chapter 4:** Present the results and the discussion of the synthesized nanocomposite.

**Chapter 5:** Focuses on the general conclusions drawn from the findings of the current research and provides recommendations for further studies.

## REFERENCES


1. Obald, J.B. and H.H. Jaber, *Eco Friendly Synthesis and Characterization of Iron Oxide Nano-Particles by Using Amaranthusspinosus Leave Extract and Apply It for Domestic Wastewater Treatment.* International Journal of Research, 2016. **3**(9): p. 665-672.
2. Qu, X., P.J. Alvarez, and Q. Li, *Applications of nanotechnology in water and wastewater treatment.* Water research, 2013. **47**(12): p. 3931-3946.
3. World Health Organization, WHO/UNICEF Joint Water Supply, & Sanitation Monitoring Programme.. Progress on sanitation and drinking water: 2015 update and MDG assessment. World Health Organization. 2015.
4. Siraj, K.T. and P.P. Rao, *Review on current world water resources scenario and water treatment technologies and techniques.* IJAR, 2016. **2**(4): p. 262-266.
5. Palamuleni, L. and M. Akoth, *Physico-chemical and microbial analysis of selected borehole water in Mahikeng, South Africa.* International journal of environmental research and public health, 2015. **12**(8): p. 8619-8630.
6. Owlad, M., Aroua, M.K., Daud, W. A.W. and Baroutian, S., Removal of hexavalent chromium-contaminated water and wastewater: a review. Water, Air, and Soil Pollution, 2009. **200**(1-4): p. 59-77.
7. Fernández-López, J.A., J.M. Angosto, and M.D. Avilés, Biosorption of hexavalent chromium from aqueous medium with opuntia biomass. The Scientific World Journal, 2014. **2014**: p. 1-8.
8. Zhitkovich, A., *Chromium in drinking water: sources, metabolism, and cancer risks.* Chemical research in toxicology, 2011. **24**(10): p. 1617-1629.
9. Costa, M., *Toxicity and carcinogenicity of Cr (VI) in animal models and humans.* Critical reviews in toxicology, 1997. **27**(5): p. 431-442.
10. Costa, M., *Potential hazards of hexavalent chromate in our drinking water.* Toxicology and applied pharmacology, 2003. **188**(1): p. 1-5.
11. Ozdemir, C., Karatas, M., Dursun, S., Argun, M.E. and Dogan, S., Effect of MnSO4 on the chromium removal from the leather industry wastewater. Environmental technology, 2005. 26(4): p. 397-400.
12. Wu, Q., Zhao, J., Qin, G., Wang, C., Tong, X., & Xue, S., Photocatalytic reduction of Cr (VI) with TiO2 film under visible light. Applied Catalysis B: Environmental, 2013. **142**: p. 142-148.
13. Anjum, M., Miandad, R., Waqas, M., Gehany, F. and Barakat, M. A., Remediation of wastewater using various nano-materials. Arabian Journal of Chemistry, 2016: p. 1-23.
14. Lauterwasser, C., Small sizes that matter: Opportunities and risks of Nanotechnologies. Report in Co-operation with the OECD International Futures Programme, 2005.
15. Saif, S., A. Tahir, and Y. Chen, *Green synthesis of iron nanoparticles and their environmental applications and implications.* Nanomaterials, 2016. **6**(11): p. 209.
16. Lakshmanan, R., Okoli, C., Boutonnet, M., Järås, S. and Rajarao, G. K., Effect of magnetic iron oxide nanoparticles in surface water treatment: Trace minerals and microbes. Bioresource technology, 2013. **129**: p. 612-615.
17. Fu, R., Zhang, X., Xu, Z., Guo, X., Bi, D. & Zhang, W., Fast and highly efficient removal of chromium (VI) using humus-supported nanoscale zero-

valent iron: Influencing factors, kinetics and mechanism. Separation and Purification Technology, 2017. **174**: p. 362-371.
18. Harman, B.I. and M. Genisoglu, Synthesis and characterization of pumice-supported nZVI for removal of copper from waters. Advances in Materials Science and Engineering, 2016. **2016**: p. 1-10.
19. Ponmani, S. and C. Udayasoorian, *Zero Valent Iron (ZVI) nanocomposite for the removal of hexavalent chromium from aqueous solution.* International Journal of Scientific and Engineering Research, 2013. **11**: p. 588-593.
20. Weng, X., Huang, L., Chen, Z., Megharaj, M. and Naidu, R., Synthesis of iron-based nanoparticles by green tea extract and their degradation of malachite. Industrial Crops and Products, 2013. **51**: p. 342-347.
21. Ismail, E., Diallo, A., Khenfouch, M., Dhlamini, S. M. and Maaza, M., RuO2 nanoparticles by a novel green process via Aspalathus linearis natural extract & their water splitting response. Journal of Alloys and Compounds, 2016. **662**: p. 283-289.
22. Carreira, C.G.L., Characterization of the Phenolic Composition of Rooibos (Aspalathus linearis) RedEspresso of the system Delta Q".
23. Safarik, I., Maderova, Z., Horska, K., Baldikova, E., Pospiskova, K. and Safarikova, M., Spent Rooibos (Aspalathus linearis) Tea Biomass as an Adsorbent for Organic Dye Removal. Bioremediation Journal, 2015. **19**(3): p. 183-187.
24. Savage, N. and M.S. Diallo, *Nanomaterials and water purification: opportunities and challenges.* Journal of Nanoparticle research, 2005. **7**(4-5): p. 331-342.
25. Mahmud, H.N.M.E., A.O. Huq, and R. binti Yahya, *The removal of heavy metal ions from wastewater/aqueous solution using polypyrrole-based adsorbents: a review.*Royal Society of Chemistry Advances, 2016. **6**(18): p. 14778-14791.
26. Barakat, M., *New trends in removing heavy metals from industrial wastewater.* Arabian Journal of Chemistry, 2011. **4**(4): p. 361-377.
27. Dixit, A., S. Dixit, and C. Goswami, *Eco-friendly alternatives for the removal of heavy metal using dry biomass of weeds and study the mechanism involved.* J. Bioremed. Biodegrad, 2015. **6**: p. 1-7.
28. Kalule-Sabiti, M. and R. Heath. *Underground water—A key resource and the associated environmental issues in the North-West Province of South-Africa*. in *Proceedings of the WISA Biennial Conference, Sun City, South Africa*. 2008.
29. Dzoma, B. M., Moralo, R. A., Motsei, L. E., Ndou, R. V. and Bakunzi, F. R., *Preliminary findings on the levels of five heavy metals in water, sediments, grass and various specimens from cattle grazing and watering in potentially heavy metal polluted areas of the North West Province of South Africa.* Journal of Animal and Veterinary Advances, 2010. **9**(24): p. 3026-3033.

# CHAPTER 2

# LITERATURE REVIEW

## 2.1 Water treatment using nanotechnology

It is estimated that 1.1 billion people lacked sufficient supply of drinking water as a result of growing population, the rising cost of potable water and variety of climatic and environmental concerns, according to World Health Organization (WHO) [1]. Nanotechnology is a significant field of modern research dealing with the design, synthesis and manipulation of particle forms with size between the range of approximately 1 – 1000 nm [2]. Nanomaterial characteristics preferable for wastewater applications include high activity for photocatalysis, antimicrobial properties for disinfection, high surface area for adsorption, super-paramagnetism for particle separation and other unique properties for water quality monitoring [3].

NPs have high surface reactivity, a large surface area available for interaction with contaminants, and could provide cost-effective solution to many challenging environmental remediation problems [4]. Table 2.1 shows different NMs that can be used in water and wastewater treatment.

**Table 2.1:** Examples of potential applications of nanotechnology in water/wastewater treatment [5]

| **Applications** | **Examples of nanomaterials** | **Some of novel properties** |
|---|---|---|
| Adsorption | CNTs/nanoscale metal oxide and nanofibers | High specific surface area and assessable adsorption sites, selective and more adsorption sites, short intraparticle diffusion distance, tunable surface chemistry, easy reuse |
| Disinfection | Nanosilver/titanium dioxide ($Ag/TiO_2$) and CNTs | Strong antimicrobial activity, low toxicity and cost, high chemical stability, ease of use |
| Photocatalysis | Nano-$TiO_2$ and Fullerene derivatives | Photocatalytic activity in solar spectrum, low human toxicity, high stability and selectivity, low cost |
| Membranes | Nano $Ag/TiO_2$/Zeolites/Magnetite and CNTs | Strong antimicrobial activity, hydrophilicity, low toxicity to humans, high mechanical and chemical stability, high permeability and selectivity, photocatalytic activity |

Various methods can be utilized for the synthesis of NPs, but these methods are broadly divided into two main classes i.e. bottom-up approach and top-down approach [6]. The top-down approach principally works with the material in its mass shape, and the size reduction to the nanoscale is then achieved by particular ablations, e.g., thermal decomposition, lithography, laser ablation, sputtering, etching, and mechanical milling[7]. In bottom-up approach, NPs can be synthesized with the use of chemical and biological techniques by self-assembling atoms to new nuclei which grow into a particle of nanoscale [8].

Lately, there has been growing interest in the synthesis of environmentally friendly NPs that do not produce toxic waste products during the production process. This can only be accomplished through mild synthesis processes of biological nature which are considered safe and environmentally safe for developing nanomaterial as an alternative to normal methods [9]. Among other methods of synthesizing NPs, plant extracts seem to be the best option[10].

## 2.2 Green synthesis

The need for safer methods of the synthesis of NPs have led to the growing interest in biological ways which are free from the use of toxic chemicals as by-products [11]. Various methods have been studied to synthesize NPs such as co-precipitation, sol-gel synthesis, micro emulsion, and the reduction of metals to NPs [12]. However, these methods are often extremely costly and not environmentally friendly because of the use of hazardous, toxic and combustible chemicals which may possibly cause environmental and biological risk as well as high energy requirement [7]. The green synthesis of NPs has been proposed as a cost-effective, environmentally friendly and can be used to substitute the chemical and physical methods [13]. Green synthesis of NPs occurs with the help of reducing and stabilizing agents [14].

Green synthesis of NPs is a form of bottom-up approach that occurs mainly via oxidation and reduction processes [15]. This method makes use of aqueous extracts with high reduction abilities, which are obtained from natural products such as tea and bush extracts [16]. Metal compounds are reduced into their respective NPs by the antioxidant and reducing properties of plant extracts [17]. Plant metabolites such as terpenoids, polyphenols, sugars, alkaloids and phenolic acids have proven to play an important role in the reduction of metal ions into NPs and in supporting their successive stability as shown in Figure 2.1 [18]. The green synthesis method requires the use of water as an environmentally friendly solvent because water is more biocompatible than organic solvents [19].

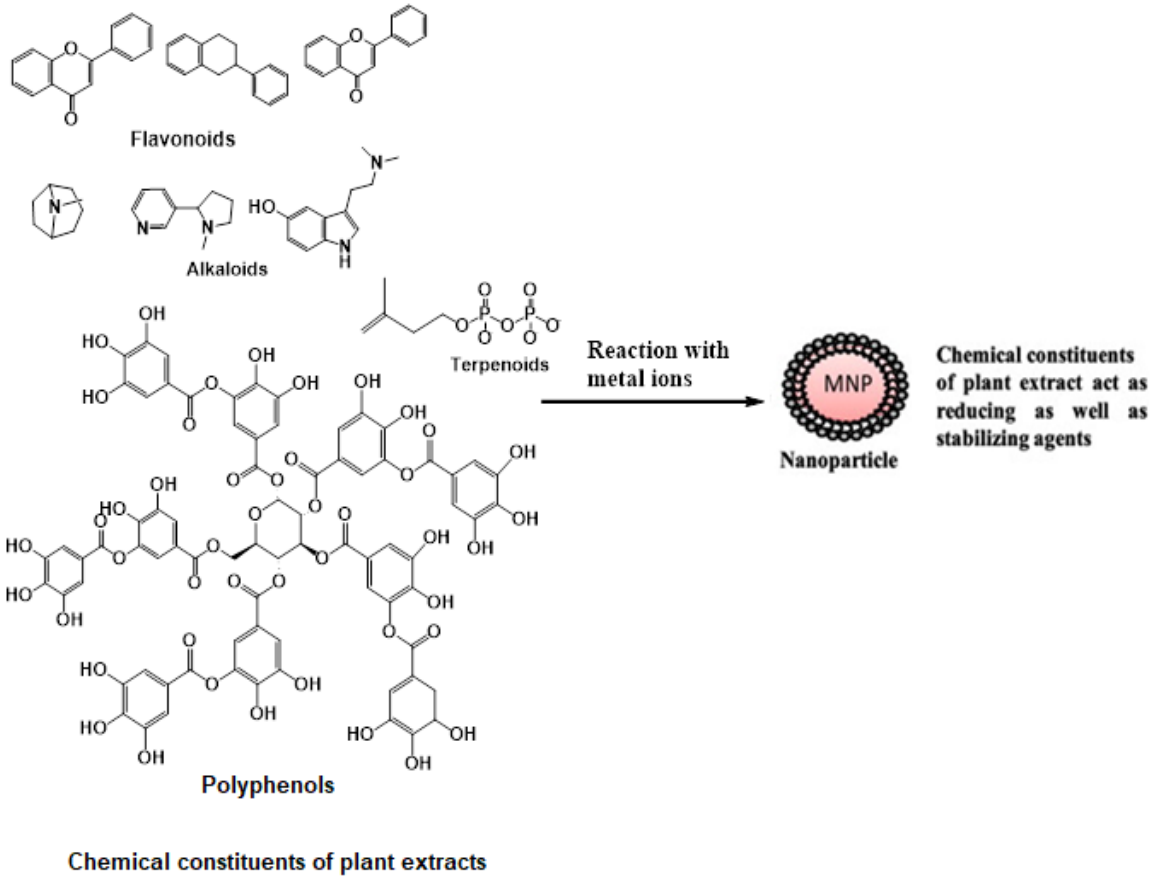


**Figure 2.1:** Synthesis of metallic NPs using plant extracts [20].

There are a number of plants that have been used to synthesize metallic NPs as presented in Table 2.2. Utilizing plants for the synthesis of NPs is emerging as an advantageous method compared to microbes because of the presence of variable bio-molecules in plants that can act as capping and reducing agents thus increasing the rate of reduction and stabilization of NPs [21]. Moreover, plant and plant derived materials eliminate the culture maintenance and are easy to handle [22].

**Table 2.2:** Plant extracts used for nanoparticles synthesis

| **Plant** | **Nanoparticle** | **Size (nm)** | **Reference** |
|---|---|---|---|
| *Allium sativum* | Ag | 12 | [23] |
| *Opuntia ficus indica* | Ag-Cu | 10 – 20 | [24] |
| Tie Guanyin tea | Fe | 6.58 ± 0.78 | [25] |
| *Aloe vera* | Au | 15.2 ± 4.2 | [26] |
| *Acalypha indica* | Ag | 20 – 30 | [27] |

## 2.3 Chemistry of Chromium

Chromium is a chemical element found in the periodic table with atomic number 24 and has symbol Cr. It is a steel-grey, hard, lustrous metal that has a high melting point (1 907℃) [28]. It is a transition element located in the group VI-B of the periodic table with a ground-state electronic configuration of Ar $3d^5 4s^1$. Louis Vauquelin who is a French chemist is first person to discover Cr in the Siberian red lead ore (crocoite) in 1798 [29]. It was named chromium (Greek chroma, “colour”) because of the various colours found in its compounds. Cr is the earth's 21st most abundant element (about 122 mg/L) and the sixth most abundant transition metal [30].

## 2.4 Chromium species

Cr can exist in several chemical forms displaying oxidation numbers from 0 to VI. However, only two of them, Cr(III) and Cr(VI) are stable enough to exist in the environment [31]. The intermediate states: Cr(II), Cr(IV), Cr(V) are unstable products in oxidation and reduction reactions of Cr(III) and Cr(VI), respectively.

Cr(III)

Cr(III) exists in natural waters as hydrolyzed $Cr(H_2O)_4OH^{2+}$ form and complexes. It is an essential micronutrient in the body and combines with various enzymes to transform protein, sugar and fat [32]. Cr(III) is strongly sorbed to mineral surfaces and sparingly soluble under acidic conditions [33]. Generally, Cr(III) compounds are relatively immobile and poorly soluble as compared to highly mobile, soluble and, consequently, more bioavailable Cr(VI) compounds [34].

Cr(VI)

Cr(VI) occurs as highly soluble and toxic chromate anions ($Cr_2O_7^{2-}$ or $HCrO_4^-$), which causes vomiting, epigastric pain, nausea, hemorrhaging, severe diarrhea and is suspected to be mutagenic and carcinogenic [35]. Cr(VI) occurs in different ionic forms ($HCrO_4^-$, $CrO_4^{2-}$ and $Cr_2O_7^{2-}$) at different pH ranges. $HCrO_4^-$ is the main form of Cr(VI) at pH < 6.0, and it converts into $CrO_4^{2-}$ with the increase in pH ( > 6.0) [36].

The species distribution of Cr(VI) in aqueous solution at different pH values is illustrated in Figure 2.2 [37].

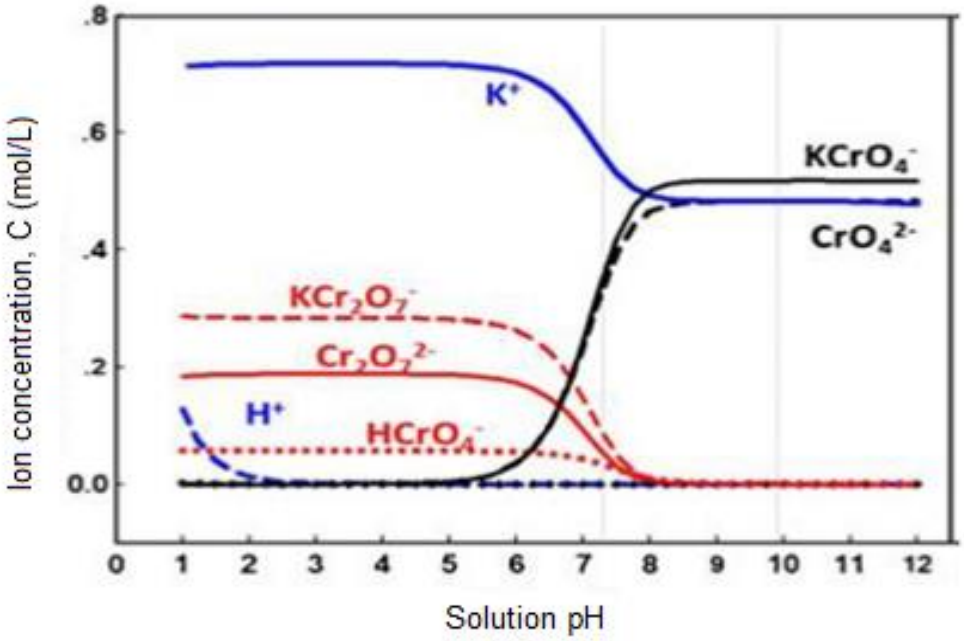


**Figure 2.2:** Cr(VI) species distribution at different pH [38].

## 2.5 Application and toxicity of chromium

Water pollution by Cr is of considerable concern, as this metal is used in various applications [39]. Cr is widely used in electroplating, metal finishing, leather tanning, nuclear power plant as well as textile industries and occurs naturally at high concentrations in ultramafic rocks, hence it is a common contaminant in surface and groundwater [40].

Cr has a potential to accumulate inside the human body and greatly affect the health of individuals. When Cr level reaches 0.1 mg/g body weight, it can ultimately become lethal [41]. United States Environmental Protection Agency (U.S EPA) has identified Cr(VI) to be one of the 17 chemicals posing great threat to human health [42]. The acceptable limit of Cr(VI) from industrial effluents to be discharged to surface and potable water is 0.1 and 0.05 mg/L, respectively [43]. According to World Health Organization (WHO), long term exposure of Cr(VI) levels of over 0.1 mg/L causes respiratory problems, liver and kidney damage [44].

## 2.6 Overview of *Asphalathus linearis*

Rooibos, *Aspalathus linearis* (Family Fabaceae; tribe Crotolarieae), is a hardy shrub that grows between 1.5 and 2 m in height with bright green, needle-shaped leaves and small, yellow flowers [45]. It is native to the Cedarberg region in the North-West of Cape Town, South Africa, where local communities have been using it for centuries to brew tea [46]. After harvesting, the needle-like leaves and stems can either be bruised and fermented before drying or can be dried immediately. The unfermented product remains green in colour and is called green rooibos. During fermentation, the colour changes from green to red with oxidation of the constituent polyphenols, so the final product is often referred to as red tea or red bush tea as shown in Figure 2.3 [47].

(a) (b) (c)

**Figure 2.3:** (a) Rooibos plant, (b) fermented rooibos leaves and (c) unfermented rooibos leaves.

The caffeine-free and relatively low tannin status of rooibos, combined with its potential health-promoting properties, most particularly antioxidant activity, contributes to its popularity [48]. Rooibos tea is not only consumed for the pleasure of its taste and aroma, but also for its medicinal properties. Rooibos has been found to alleviate dermatological problems, allergies, asthma, infantile colic and other gastrointestinal complaints, such as nausea and heartburn [49]. It is usually used for children suffering from allergic skin conditions, such as eczema and nappy rash. Rooibos tea is believed to increase appetite, therefore, it is very popular among mothers whose babies have difficulty breastfeeding in some of the rural black communities in South Africa [50]. As depicted in Figure 2.4, rooibos extract contains

among others, two unique phenolic compounds, namely dihydrochalcone C-glucoside, aspalathin, aspalalinin and a cyclic dihydrochalcone [51].

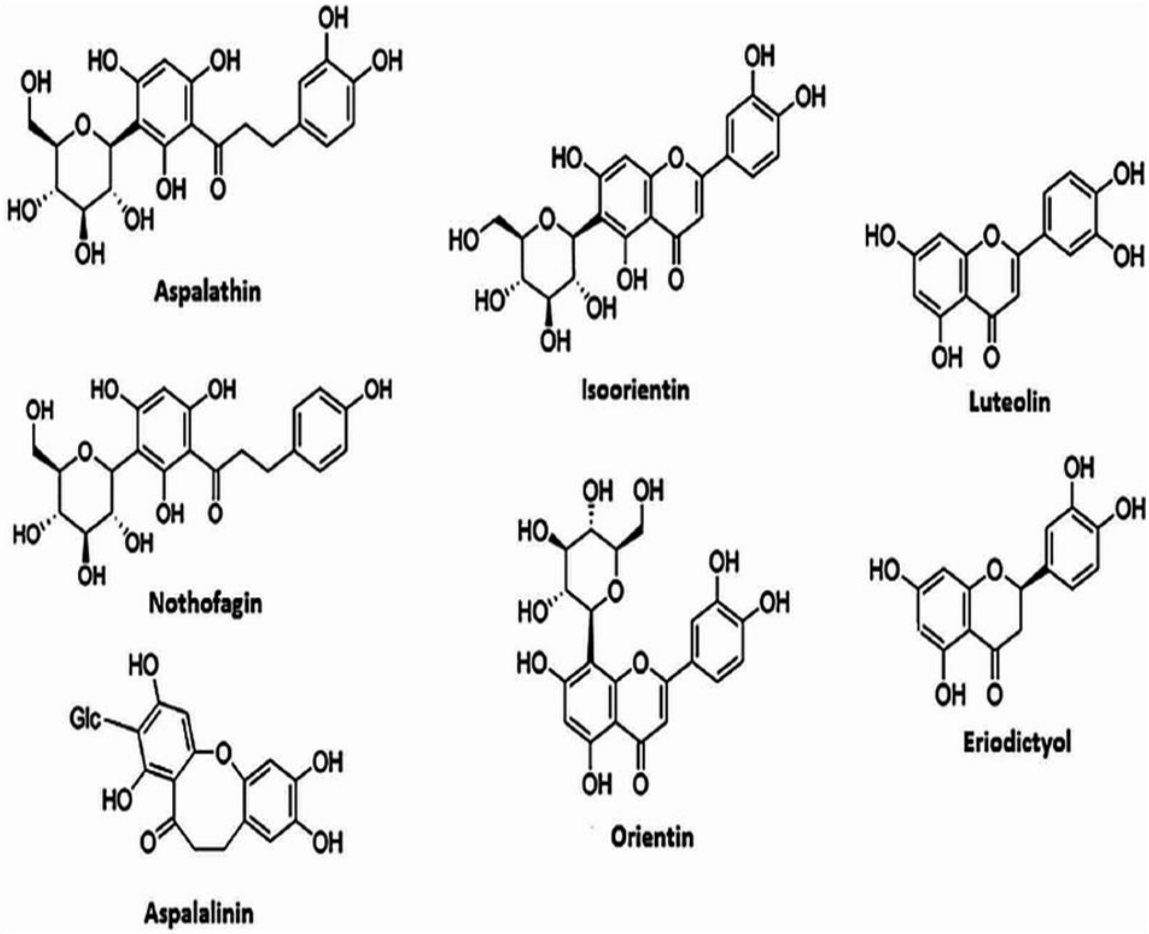


**Figure 2.4:** Some of the major bioactive molecular compounds within the rooibos extract [52].

Kanu *et al*. [53] studied the biosorption of Pb(II) using rooibos shoot powder (RSP). The effect of experimental parameters such as solution pH, initial Pb(II) concentration, contact time, adsorbent dosage and temperature were investigated on biosorption process. The results showed that pH 6.7 was the most favourable and that biosorption uptake decreased with increasing biosorbent dosage and increased with increasing Pb(II) concentration. The outcomes from this analysis showed that RSP may be used as an eco-friendly, low-cost, and effective biosorbent for the removal of Pb(II) from environmental wastewaters.

## 2.7 Choice of polymer

Conducting polymers such as polyaniline, polypyrrole, polythiophene, etc. have attracted considerable attention in many applications [54]. Recently, researchers pay their attention on Ppy in adsorption due to its useful properties for adsorbent synthesis, good environmental stability, non-toxic nature, good biocompatibility and relatively low cost [55]. Ppy is poorly dispersed in water and has a the tendency to agglomerate in irregular morphology, which occasionally reduces the surface area, hence, some researchers have focussed on the fabrication of nanostructured Ppy or Ppy based NCs with large surface area for highly efficient removal of contaminants from water [56]. Ppy offers a good potential for its applications in adsorption or filtration separation due to the existence of positively charged nitrogen atoms as shown in Figure 2.5 [57]. To maintain charge neutrality, some of the counter anions present in the polymerization solution are incorporated into the growing polymer during the polymerization [58].

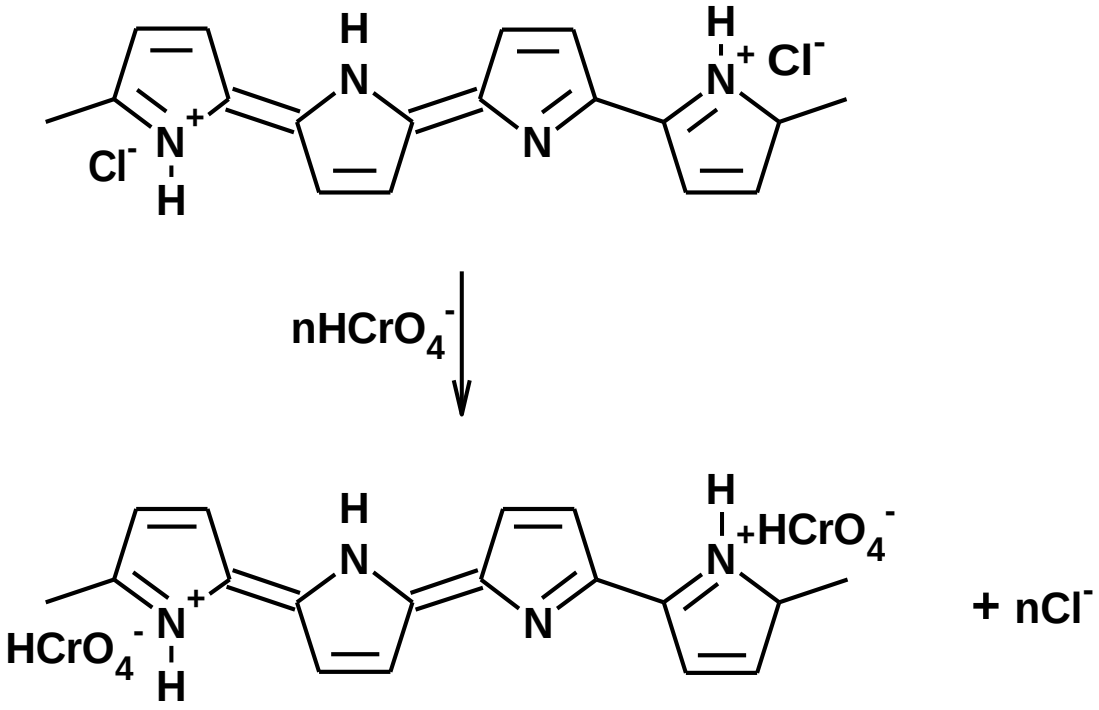


**Figure 2.5:** A probable mechanism for the removal of Cr(VI) ions from aqueous solution [59].

Figure 2.6 depicts that when Ppy is treated with an acid or alkali solution, it can proceed in protonation or deprotonation processes, resulting in doping or dedoping of counter ion. As a consequence of reversible transformation capability, adsorbents

based on Ppy can be regenerated in the adsorption process [60]. The ability of Ppy to reversibly change between its charged and neutral state has made it possible for it to be used as a functional material in the manufacture of ion-selective membranes, in the making of pH sensors and biosensor [58].

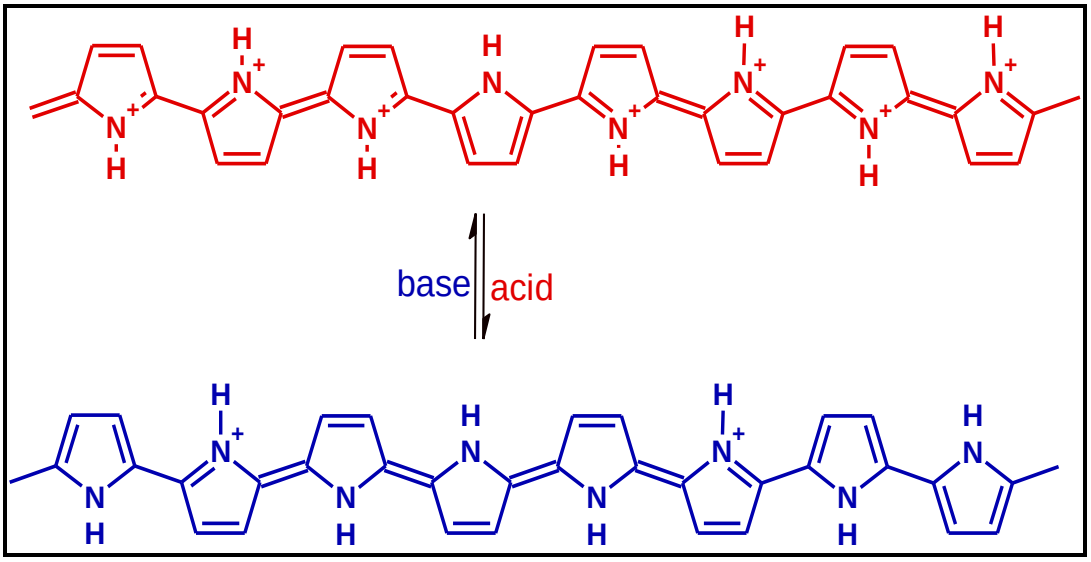


**Figure 2.6:** Protonation/deprotonation technique of Ppy [61].

### 2.8 Adsorption as an efficient method for removing pollutants

Adsorption is a mass transfer process which involves the accumulation of substances at the mixing of two phases, such as, liquid–liquid, gas–solid, gas–liquid, or liquid–solid interface [62] and becomes bound by physical and/or chemical interactions. It is a partition process in which few components of the liquid phase are relocated to the surface of the solid adsorbents [63]. The solute retained (on the solid surface) in adsorption processes is called adsorbate, while the solid on which it is retained is called as an adsorbent [64]. The properties of adsorbates and adsorbents are quite specific and depend upon their constituents. The constituents of adsorbents are mainly responsible for the removal of any particular pollutants from wastewater [65]. Since adsorption is a surface phenomenon, nanoadsorbents offer high sorption efficiency and rapid process kinetics due to their large surface area and easily accessible sorption sites [66].

Many treatment techniques such as adsorption, ion-exchange, membrane separation, electrodialysis and chemical precipitation (Figure 2.7) have been applied

for the elimination of Cr(VI) from aqueous solutions [67]. Despite their high efficiency and usefulness, these techniques also have some disadvantages that limit the application, such as considerable toxic waste production, high cost, and huge energy consumption [68]. Among them, adsorption is the most cost-efficient and a promising method due to its simplicity, flexibility and high efficiency in industrial application [69]. Adsorption method relies on several materials for decontaminating water, commonly used adsorbents are activated carbon, chitosan, zeolite and clay minerals [70].

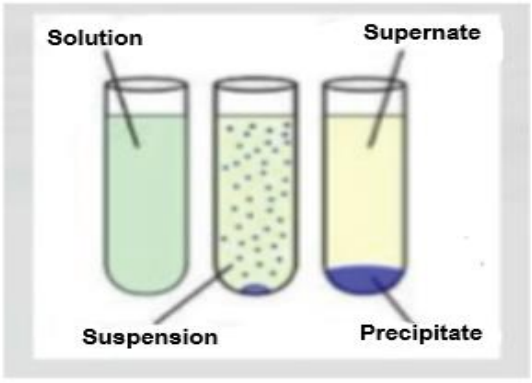


**Precipitation**

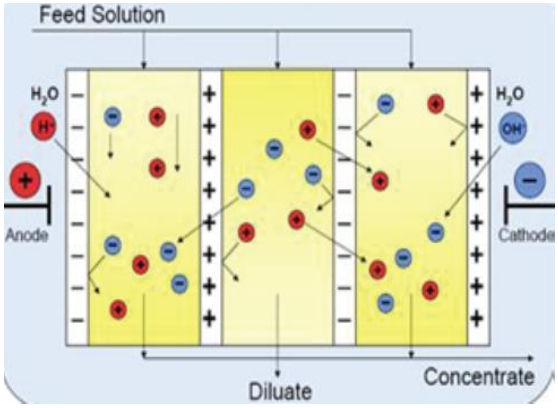


**Electrodialysis**

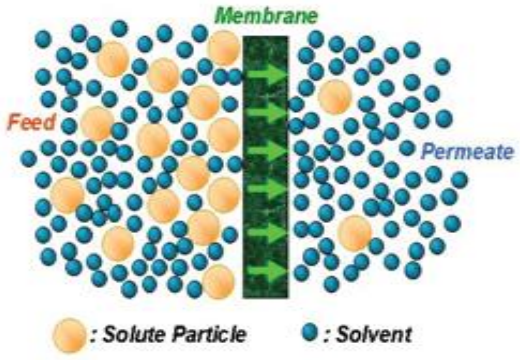


**Membrane separation**

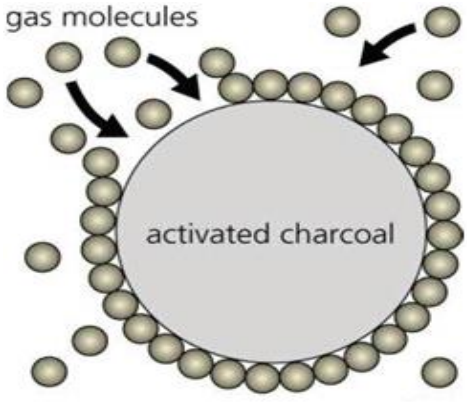


**Adsorption**

**Figure 2.7:** Some of the methods for pollutant removal [71].

The constituents of adsorbents are mainly responsible for the removal of any particular pollutants from wastewater [72]. The mechanism of adsorption is divided

into three steps (a) diffusion of adsorbate to adsorbent surface, (b) migration into pores of adsorbent and (c) monolayer build-up of adsorbate on the adsorbent. Figure 2.8 presents the process of adsorbate distribution. Adsorption mechanism starts by the diffusion of adsorbate on the adsorbent surface through intermolecular forces between adsorbate and adsorbent. The second step includes migration of adsorbate into pores of adsorbent. In the last step, when the adsorbate's particles are distributed on the surface and filled up the volume of pores, particles of adsorbate are building up the monolayer of reacted molecules, ions and atoms to the active sites of adsorbent [73].

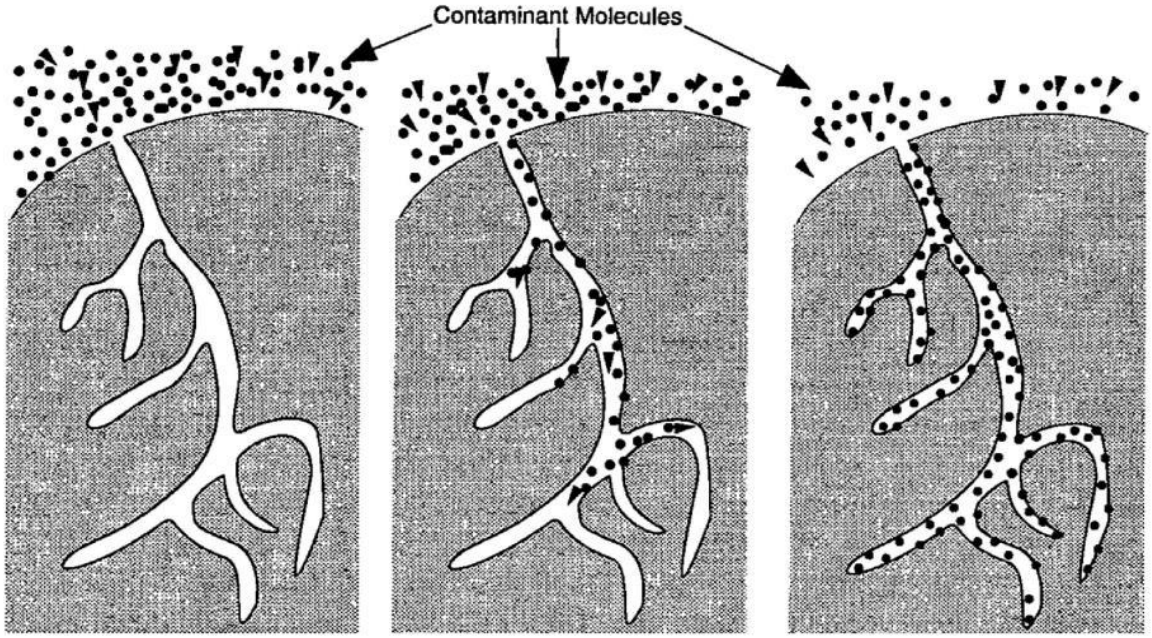


**Figure 2.8:** Adsorption mechanism [73].

Factors affecting the adsorption process are:

- initial concentration of adsorbate
- solution pH
- temperature
- surface area
- dose of adsorbent [72].

## 2.9 Adsorption isotherm models

An adsorption isotherm is an invaluable curve describing the phenomenon controlling the release or mobility of a substance from the aqueous porous media or aquatic environments to a solid-phase at a constant temperature and pH [74]. The adsorption isotherm is a fundamental source of information on the adsorption process. The analytical forms of adsorption isotherm equations depend on the type of the surface phase that can be considered as a monolayer or multilayer, and as localized, mobile [75]. The connection between adsorbate and adsorbent can be explained by adsorption isotherms and provides the parameter for designing a desired adsorption isotherm model [76].

Equilibrium studies determine the capacity of the adsorbent and describe the adsorption isotherm by constants which values express the surface properties as well as affinity of the adsorbents. The relationship between equilibrium data and either theoretical or practical equations is important for interpretation and prediction of the extent of adsorption [77]. Langmuir and Freundlich models are the most commonly used adsorption isotherms even though they were first introduced over 90 years ago [78].

### 2.9.1 Langmuir isotherm model

The Langmuir isotherm assumes that adsorption occurs at specific homogeneous sites within the adsorbent without any interaction between the adsorbed substances [79]. Graphically, a plateau distinguishes the Langmuir isotherm. Therefore, at equilibrium, a saturation point is reached where no further adsorption can occur [80]. Once a site is filled, no further sorption can take place at that site. As such the surface will eventually reach a saturation point where the maximum adsorption of the surface will be achieved [81]. The linear form of the Langmuir isotherm is described in Eqn. (1):

$$\frac{C_e}{q_e} = \frac{C_e}{q_m} + \frac{1}{K_L q_m} \quad (1)$$

Where $q_m$ is the maximum adsorption capacity (mg/g) and $K_L$ is a Langmuir constant related to the energy of adsorption [82]. A further analysis of the Langmuir equation

can be made on the basis of a limitless equilibrium parameter, $R_L$, also known as the separation factor, given by Eqn. (2):

$$R_L = \frac{1}{1+bC_0} \quad (2)$$

### 2.9.2 Freundlich isotherm model

The Freundlich isotherm gives an expression which defines the surface heterogeneity and the exponential distribution of active sites and their energies [83]. This model is considered to be appropriate for describing both multilayer adsorption and adsorption on heterogeneous surfaces [84]. The linear form of the Freundlich isotherm is as in Eqn. (3):

$$\log q_e = \log K_f \frac{1}{n} \log C_e \quad (3)$$

where *n* is the heterogeneity factor denoting the adsorption intensity and $K_F$ [L/g(mg/L)$^{-1/n}$] is the Freundlich constant [85].

## 2.10 Kinetic models

Kinetics is the study of the rate of chemical processes to understand the factors that influence the rate. Chemical kinetics study includes careful monitoring of the experimental conditions which influence the speed of a chemical reaction and hence, help achieve equilibrium in a reasonable length of time [86]. The kinetic parameters are useful in predicting the adsorption rate which can be used as important information in designing and modelling of the adsorption operation. The kinetics of removal of metal ions is fully explained in the literature using pseudo-first-order and pseudo-second-order kinetic models [87].

### 2.10.1 Pseudo-first order

Lagergren described liquid–solid phase adsorption systems which consisted of the adsorption of oxalic acid and malonic acid onto charcoal as early as 1898 [88]. The kinetic data were treated with the Lagergren first-order model, which is the earliest known one describing the adsorption rate based on the adsorption capacity [89]. Lagergren pseudo-first order kinetic model is mathematically expressed by Eqn. (4):

$$\log (q_e - q_t) = \log q_e - \frac{K_1}{2.303} t \quad (4)$$

where, $q_e$ and $q_t$ are the amounts of adsorbed Cr(VI) (mg/g) at equilibrium and at time t (min), respectively, and $k_1$ (1/min) is the adsorption rate constant of pseudo-first order kinetic model [90].

### 2.10.2 Pseudo-second order

In study of adsorption kinetics, pseudo-second order kinetic equation has been most widely used to describe time evolution of adsorption under non equilibrium conditions [91]. Pseudo-second order kinetic model is given by Eqn. (5):

$$\frac{t}{qt} = \frac{1}{K_2 q_e^2} + \frac{1}{q_e} \quad (5)$$

where $q_t$ is Cr(VI) uptake at time t, and $k_2$ is the second order rate constant. From pseudo second kinetic model, the initial sorption rate, $h_0$ (mg/g/min) can be defined by Eqn. (6) [92]:

$$h_0 = k_2 q_e^2 \ (t \rightarrow 0) \quad (6)$$

## 2.11 Current research approach

A number of studies have been done on Ppy NC for removal of pollutants in water. Some of them are discussed below.

In a study by Bhaumik *et al*. [93] Ppy/$Fe_3O_4$ magnetic nanocomposite was synthesized via *in-situ* oxidative polymerization of Py monomer using $FeCl_3$ oxidant in aqueous medium in which $Fe_3O_4$ NPs were suspended. Up to 97% of the adsorbed fluoride on the Ppy/$Fe_3O_4$ NC was desorbed at pH 2. The adsorbent retained the original adsorption capacity after one complete adsorption-desorption cycle, confirming the reusability of the NC for fluoride removal.

Setshedi *et al*. [94] prepared exfoliated polypyrrole-organically modified montmorillonite clay nanocomposite via *in-situ* polymerization of Py monomer for adsorption of toxic Cr(VI) from aqueous solution. The study revealed that adsorption of Cr(VI) increased with an increase in temperature and optimum Cr(VI) removal was

achieved at pH 2. Langmuir adsorption isotherm model fitted the data well and the maximum adsorption capacity was found to be 119.34 mg/g at 298 K.

Kera *et al*. [95] reported 100% Cr(VI) removal at pH 2 using Ppy-PANI/$Fe_3O_4$ NC. The study revealed that co-existing ions did not affect Cr(VI) removal and that the NC was highly selective in the presence of other cations and anions. It was concluded that the incorporation of $Fe_3O_4$ NPs into Ppy-PANI NC resulted in a reusable magnetic adsorbent with a high adsorption capacity and selectivity for Cr(VI).

## 2.12 Concluding remarks

The literature reviewed herein has revealed that the traditional methods of synthesizing NMs for heavy metal contamination using chemical and physical methods have drawbacks such as production of toxic by-products and being expensive. It is for that reason that the cost-effective and environmentally friendly method of developing NC for Cr(VI) is of utmost importance.

## REFERENCES


1. Anjum, M., Miandad, R., Waqas, M., Gehany, F. and Barakat, M. A., Remediation of wastewater using various nano-materials. Arabian Journal of Chemistry, 2016. p. 1-23.
2. Amargeetha, A. and S. Velavan, *Green Synthesis of Silver Nanoparticle using Erythrina indica Flower Extract.* Journal of Nanoscience and Technology, 2017: p. 293-295.
3. Qu, X., Brame, J., Li, Q., & Alvarez, P. J., Nanotechnology for a safe and sustainable water supply: enabling integrated water treatment and reuse. Accounts of Chemical Research, 2012. **46**(3): p. 834-843.
4. Jahin, H.S., Fluoride removal from water using nanoscale zero-valent iron (NZVI). International Water Technology Journal, 2014. **4**: p. 173-182.
5. Amin, M., A. Alazba, and U. Manzoor, A review of removal of pollutants from water/wastewater using different types of nanomaterials. Advances in Materials Science and Engineering, 2014. **2014**.
6. Khan, I., K. Saeed, and I. Khan, Nanoparticles: Properties, applications and toxicities. Arabian Journal of Chemistry, 2017.
7. Keat, C. L., Aziz, A., Eid, A. M. and Elmarzugi, N. A., Biosynthesis of nanoparticles and silver nanoparticles. Bioresources and Bioprocessing, 2015. **2**(1): p. 47.
8. Ahmed, S., Ahmad, M., Swami, B. L. and Ikram, S., A review on plants extract mediated synthesis of silver nanoparticles for antimicrobial applications: a green expertise. Journal of Advanced Research, 2016. **7**(1): p. 17-28.
9. Chauhan, R.P., C. Gupta, and D. Prakash, *Methodological advancements in green nanotechnology and their applications in biological synthesis of herbal nanoparticles.* International Journal of Bioassays, 2012. **1**(7): p. 6-10.
10. Ahmad, N. and S. Sharma, *Green synthesis of silver nanoparticles using extracts of Ananas comosus.* Green and Sustainable Chemistry, 2012. **2**(04): p. 141.
11. Singhal, G., Bhavesh, R., Kasariya, K., Sharma, A. R. and Singh, R. P., Biosynthesis of silver nanoparticles using Ocimum sanctum (Tulsi) leaf extract and screening its antimicrobial activity. Journal of Nanoparticle Research, 2011. **13**(7): p. 2981-2988.
12. Ehrampoush, M. H., Miria, M., Salmani, M. H. and Mahvi, A. H., Cadmium removal from aqueous solution by green synthesis iron oxide nanoparticles with tangerine peel extract. Journal of Environmental Health Science and Engineering, 2015. 13(1): p. 84.13. Prasad, C., S. Gangadhara, and P. Venkateswarlu, *Bio-inspired green synthesis of Fe3O4 magnetic nanoparticles using watermelon rinds and their catalytic activity.* Applied Nanoscience, 2016. **6**(6): p. 797-802.
14. Patra, J.K. and K.-H. Baek, *Green nanobiotechnology: factors affecting synthesis and characterization techniques.* Journal of Nanomaterials, 2014. **2014**: p. 219.
15. Yuvaraj, D., L. Christudhas, and K. Ramesh, *Bio-Synthesis of Iron Nanoparticles using the Brown Seaweed, Dictyota dicotoma.* BioTechnology: An Indian Journal, 2016. **12**(12).
16. Machado, S., Pacheco, J. G., Nouws, H. P. A., Albergaria, J. T. and Delerue-Matos, C., Characterization of green zero-valent iron nanoparticles produced with tree leaf extracts. Science of The Total Environment, 2015. **533**: p. 76-81.

17. Pattanayak, M. and P. Nayak, *Green synthesis and characterization of zero valent iron nanoparticles from the leaf extract of Azadirachta indica (Neem).*World Journal of Nano Science and Technology, 2013. **2**(1): p. 06-09.
18. Makarov, V. V., Love, A. J., Sinitsyna, O. V., Makarova, S. S., Yaminsky, I. V., Taliansky, M. E. and Kalinina, N. O., “Green” nanotechnologies: synthesis of metal nanoparticles using plants. Acta Naturae (англоязычная версия), 2014. **6** (20): p. 35-44.
19. Park, Y., *New paradigm shift for the green synthesis of antibacterial silver nanoparticles utilizing plant extracts.* Toxicological research, 2014. **30**(3): p. 169.
20. Mittal, A.K., Y. Chisti, and U.C. Banerjee, *Synthesis of metallic nanoparticles using plant extracts.* Biotechnology advances, 2013. **31**(2): p. 346-356.
21. Singh, S., GREEN NANOBIOTECHNOLOGY-AN OVERVIEW OF SYNTHESIS, CHRACTERISATION AND APPLICATIONS. 2016. **5**(8): p. 501-531.
22. Vanaja, M., Paulkumar, K., Baburaja, M., Rajeshkumar, S., Gnanajobitha, G., Malarkodi, C., Sivakavinesan, M. and Annadurai, G., Degradation of methylene blue using biologically synthesized silver nanoparticles. Bioinorganic Chemistry and Applications, 2014. **2014**.
23. Ahamed, M., Khan, M. M., Siddiqui, M. K. J., AlSalhi, M. S. and Alrokayan, S. A., Green synthesis, characterization and evaluation of biocompatibility of silver nanoparticles. Physica E: Low-dimensional Systems and Nanostructures, 2011. 43(6): p. 1266-1271.
24. Rocha-Rocha, O., Cortez-Valadez, M., Hernández-Martínez, A.R., Gámez-Corrales, R., Alvarez, R.A., Britto-Hurtado, R., Delgado-Beleño, Y., Martinez-Nuñez, C.E., Pérez-Rodríguez, A., Arizpe-Chávez, H. and Flores-Acosta, M., Green Synthesis of Ag-Cu Nanoalloys Using Opuntia ficus-indica. Journal of Electronic Materials, 2017. **46**(2): p. 802-807.
25. Xin, H., Yang, X., Liu, X., Tang, X., Weng, L. and Han, Y., Biosynthesis of Iron Nanoparticles Using Tie Guanyin Tea Extract for Degradation of Bromothymol Blue. Journal of Nanotechnology, 2016. **2016**.
26. Chandran, S.P., Chaudhary, M., Pasricha, R., Ahmad, A. and Sastry, M., Synthesis of gold nanotriangles and silver nanoparticles using Aloevera plant extract. Biotechnology Progress, 2006. **22**(2): p. 577-583.
27. Krishnaraj, C., Jagan, E.G., Rajasekar, S., Selvakumar, P., Kalaichelvan, P.T. and Mohan, N., Synthesis of silver nanoparticles using Acalypha indica leaf extracts and its antibacterial activity against water borne pathogens. Colloids and Surfaces B: Biointerfaces, 2010. **76**(1): p. 50-56.
28. Owlad, M., Aroua, M.K., Daud, W.A.W. and Baroutian, S., Removal of hexavalent chromium-contaminated water and wastewater: a review. Water, Air, and Soil Pollution, 2009. **200**(1-4): p. 59-77.
29. Shanker, A.K., Cervantes, C., Loza-Tavera, H. and Avudainayagam, S., Chromium toxicity in plants. Environment International, 2005. **31**(5): p. 739-753.
30. Mohan, D. and C.U. Pittman Jr, *Activated carbons and low cost adsorbents for remediation of tri-and hexavalent chromium from water.* Journal of hazardous materials, 2006. **137**(2): p. 762-811.
31. Kotaś, J. and Z. Stasicka, *Chromium occurrence in the environment and methods of its speciation.* Environmental pollution, 2000. **107**(3): p. 263-283.

32. Gomez, V. and M. Callao, *Chromium determination and speciation since 2000.* TrAC Trends in Analytical Chemistry, 2006. **25**(10): p. 1006-1015.
33. Izbicki, J.A., Wright, M.T., Seymour, W.A., McCleskey, R.B., Fram, M.S., Belitz, K. and Esser, B.K., Cr (VI) occurrence and geochemistry in water from public-supply wells in California. Applied Geochemistry, 2015. **63**: p. 203-217.
34. Markiewicz, B., Komorowicz, I., Sajnóg, A., Belter, M. and Barałkiewicz, D., Chromium and its speciation in water samples by HPLC/ICP-MS–technique establishing metrological traceability: A review since 2000. Talanta, 2015. **132**: p. 814-828.
35. Xu, X., Gao, B.Y., Tan, X., Yue, Q.Y., Zhong, Q.Q. and Li, Q., Characteristics of amine-crosslinked wheat straw and its adsorption mechanisms for phosphate and chromium (VI) removal from aqueous solution. Carbohydrate polymers, 2011. **84**(3): p. 1054-1060.
36. Santhosh, C., Nivetha, R., Kollu, P., Srivastava, V., Sillanpää, M., Grace, A.N. and Bhatnagar, A., Removal of cationic and anionic heavy metals from water by 1D and 2D-carbon structures decorated with magnetic nanoparticles. Scientific reports, 2017. **7**(1): p. 14107.
37. Ilankoon, N., *Use of iron oxide magnetic nanosorbents for Cr (VI) removal from aqueous solutions: A review.* Journal of Engineering Research and Applications, 2014. **4**: p. 55-63.
38. Chen, R., Chai, L., Li, Q., Shi, Y., Wang, Y. and Mohammad, A., Preparation and characterization of magnetic Fe3O4/CNT nanoparticles by RPO method to enhance the efficient removal of Cr (VI). Environmental Science and Pollution Research, 2013. **20**(10): p. 7175-7185.
39. Garg, U.K., Kaur, M.P., Garg, V.K. and Sud, D., Removal of hexavalent chromium from aqueous solution by agricultural waste biomass. Journal of Hazardous materials, 2007. **140**(1-2): p. 60-68.
40. Shen, H., Chen, J., Dai, H., Wang, L., Hu, M. and Xia, Q., New insights into the sorption and detoxification of chromium (VI) by tetraethylenepentamine functionalized nanosized magnetic polymer adsorbents: mechanism and pH effect. Industrial & Engineering Chemistry Research, 2013. **52**(36): p. 12723-12732.
41. Fazlzadeh, M., Rahmani, K., Zarei, A., Abdoallahzadeh, H., Nasiri, F. and Khosravi, R., A novel green synthesis of zero valent iron nanoparticles (NZVI) using three plant extracts and their efficient application for removal of Cr (VI) from aqueous solutions. Advanced Powder Technology, 2017. **28**(1): p. 122-130.
42. Cheung, K. and J.-D. Gu, *Mechanism of hexavalent chromium detoxification by microorganisms and bioremediation application potential: a review.* International Biodeterioration & Biodegradation, 2007. **59**(1): p. 8-15.
43. Ballav, N., A. Maity, and S.B. Mishra, *High efficient removal of chromium (VI) using glycine doped polypyrrole adsorbent from aqueous solution.* Chemical engineering journal, 2012. **198**: p. 536-546.
44. Anah, L.; Astrini, N. Influence of pH on Cr(VI) ions removalfrom aqueous solutions using carboxymethyl cellulose-based hydrogel as adsorbent. IOP Conf. Ser. Earth and Environmental Sciences 2017, **60**, 012010.
45. Ajuwon, O.R., J.L. Marnewick, and L.M. Davids, Rooibos (Aspalathus linearis) and its Major Flavonoids—Potential Against Oxidative Stress-Induced Conditions, in Basic Principles and Clinical Significance of Oxidative Stress. 2015. p 171-218.

46. Kanu, S. A., Moyo, M., Khamlich, S. and Okonkwo, J. O., Adsorption of cadmium from aqueous solution using Rooibos shoots as adsorbent. Toxicological and Environmental Chemistry, 2014. **96**(10): p. 1452-1462.
47. McKay, D.L. and J.B. Blumberg, *A review of the bioactivity of South African herbal teas: rooibos (Aspalathus linearis) and honeybush (Cyclopia intermedia).* Phytotherapy Research, 2007. **21**(1): p. 1-16.
48. Joubert, E. and D. de Beer, *Rooibos (Aspalathus linearis) beyond the farm gate: From herbal tea to potential phytopharmaceutical.* South African Journal of Botany, 2011. **77**(4): p. 869-886.
49. Hübsch, Z., S. Van Vuuren, and R. Van Zyl, *Can rooibos (Aspalathus linearis) tea have an effect on conventional antimicrobial therapies?* South African Journal of Botany, 2014. **93**: p. 148-156.
50. Van Niekerk, C. and A. Viljoen, *Indigenous South African medicinal plants part 11: Aspalathus linearis ('Rooibos'): medicinal plants.* SA Pharmaceutical Journal, 2008. **75**(10): p. 41-42.
51. Diallo, A., et al., *Green synthesis of ZnO nanoparticles by Aspalathus linearis: Structural & optical properties.* Journal of Alloys and Compounds, 2015. **646**: p. 425-430.
52. Diallo, A., et al., *Physical & enhanced photocatalytic properties of green synthesized SnO2 nanoparticles via Aspalathus linearis.* Journal of Alloys and Compounds, 2016. **681**: p. 561-570.
53. Kanu, S.A., et al., *Biosorption of Pb (II) from aqueous solution using Rooibos shoot powder (RSP).* Desalination and Water Treatment, 2016. **57**(12): p. 5614-5622.
54. Chen, J., J. Feng, and W. Yan, *Facile synthesis of a polythiophene/$TiO_2$ particle composite in aqueous medium and its adsorption performance for Pb(ii).* RSC Advances, 2015. **5**(106): p. 86945-86953.
55. Chen, J., Shu, C., Wang, N., Feng, J., Ma, H., & Yan, W., Adsorbent synthesis of polypyrrole/TiO2 for effective fluoride removal from aqueous solution for drinking water purification: Adsorbent characterization and adsorption mechanism. Journal of Colloid and Interface Science, 2017. **495**: p. 44-52.
56. Setshedi, K. Z., Bhaumik, M., Onyango, M. S., & Maity, A., High-performance towards Cr(VI) removal using multi-active sites of polypyrrole–graphene oxide nanocomposites: batch and column studies. Chemical Engineering Journal, 2015. **262**: p. 921-931.
57. Bhaumik, M., Maity, A., Srinivasu, V. V. and Onyango, M. S., Enhanced removal of Cr(VI) from aqueous solution using polypyrrole/Fe3O4 magnetic nanocomposite. Journal of hazardous materials, 2011. **190**(1): p. 381-390.
58. Zhang, X. and R. Bai, *Surface electric properties of polypyrrole in aqueous solutions.* Langmuir, 2003. **19**(26): p. 10703-10709.
59. Mahmud, H.N.M.E., A.O. Huq, and R. binti Yahya, The removal of heavy metal ions from wastewater/aqueous solution using polypyrrole-based adsorbents: a review. Royal Society of Chemistry Advances, 2016. **6**(18): p. 14778-14791.
60. Chen, J., J. Feng, and W. Yan, *Influence of metal oxides on the adsorption characteristics of PPy/metal oxides for Methylene Blue.*Journal of Colloid and Interface Science, 2016. **475**: p. 26-35.
61. Liao, S., Xue, C., Wang, Y., Zheng, J., Hao, X., Guan, G., Abuliti, A., Zhang, H. and Ma, G., Simultaneous separation of iodide and cesium ions from dilute

wastewater based on PPy/PTCF and NiHCF/PTCF electrodes using electrochemically switched ion exchange method. Separation and Purification Technology, 2015. **139**: p. 63-69.
62. De Gisi, S., Lofrano, G., Grassi, M. and Notarnicola, M., Characteristics and adsorption capacities of low-cost sorbents for wastewater treatment: a review. Sustainable Materials and Technologies, 2016. **9**: p. 10-40.
63. Tripathi, A. and M.R. Ranjan, *Heavy metal removal from wastewater using low cost adsorbents.*Journal of Bioremediation and Biodegradation, 2015. **6**: p. 315.
64. Rashed, M.N., Adsorption technique for the removal of organic pollutants from water and wastewater, in Organic pollutants-monitoring, risk and treatment. 2013. p. 167–194.
65. Khattri, S. and M. Singh, *Removal of malachite green from dye wastewater using neem sawdust by adsorption.* Journal of Hazardous Materials, 2009. **167**(1-3): p. 1089-1094.
66. Bhaumik, M., Setshedi, K., Maity, A. and Onyango, M.S., Chromium (VI) removal from water using fixed bed column of polypyrrole/$Fe_3O_4$ nanocomposite. Separation and Purification Technology, 2013. **110**: p. 11-19.
67. Soliemanzadeh, A. and M. Fekri, *The application of green tea extract to prepare bentonite-supported nanoscale zero-valent iron and its performance on removal of Cr (VI): Effect of relative parameters and soil experiments.* Microporous and Mesoporous Materials, 2017. **239**: p. 60-69.
68. Chen, T., Zhou, Z., Xu, S., Wang, H. and Lu, W., Adsorption behavior comparison of trivalent and hexavalent chromium on biochar derived from municipal sludge. Bioresource Technology, 2015. **190**: p. 388-394.
69. Wang, T., Liu, W., Xiong, L., Xu, N. and Ni, J., Influence of pH, ionic strength and humic acid on competitive adsorption of Pb(II), Cd(II) and Cr(III) onto titanate nanotubes. Chemical Engineering Journal, 2013. **215**: p. 366-374.
70. Yua, C. and X. Han, Adsorbent Material Used In Water Treatment-A Review. In 2nd International Workshop on Materials Engineering and Computer Sciences IWMECS. 2015. p. 290-293.
71. Abdel-Raouf, M. and A. Abdul-Raheim, Removal of Heavy Metals from Industrial Waste Water by Biomass-Based Materials: A Review. Journal of Pollution Effects and Control, 2017. **5**: p. 180.
72. Grassi, M., Kaykioglu, G., Belgiorno, V. and Lofrano, G., Removal of emerging contaminants from water and wastewater by adsorption process, in Emerging compounds removal from wastewater. Springer, 2012,. p. 15-37.
73. Musin, E.,Thesis: Adsorption Modelling.Mikkeli University of Applied Science 2013.
74. Foo, K. and B. Hameed, *Insights into the modeling of adsorption isotherm systems.* Chemical Engineering Journal, 2010. **156**(1): p. 2-10.
75. S Saadi, R., Saadi, Z., Fazaeli, R. and Fard, N.E., Monolayer and multilayer adsorption isotherm models for sorption from aqueous media. Korean Journal of Chemical Engineering, 2015. **32**(5): p. 787-799.
76. Poguberović, S.S., Krčmar, D.M., Maletić, S.P., Kónya, Z., Pilipović, D.D.T., Kerkez, D.V. and Rončević, S.D., Removal of As(III) and Cr(VI) from aqueous solutions using “green” zero-valent iron nanoparticles produced by oak, mulberry and cherry leaf extracts. Ecological Engineering, 2016. **90**: p. 42-49.

77. Vimonses, V., Lei, S., Jin, B., Chow, C.W. and Saint, C., Kinetic study and equilibrium isotherm analysis of Congo Red adsorption by clay materials. Chemical Engineering Journal, 2009. **148**(2-3): p. 354-364.
78. Repo, E., Thesis: EDTA-and DTPA-functionalized silica gel and chitosan adsorbents for the removal of heavy metals from aqueous solutions. Lappeenranta University of Technology. 2011.
79. Iakovleva, E. and M. Sillanpää, *The use of low-cost adsorbents for wastewater purification in mining industries.* Environmental Science and Pollution Research, 2013. **20**(11): p. 7878-7899.
80. Allen, S., G. Mckay, and J.F. Porter, *Adsorption isotherm models for basic dye adsorption by peat in single and binary component systems.* Journal of colloid and interface science, 2004. **280**(2): p. 322-333.
81. Boparai, H.K., M. Joseph, and D.M. O'Carroll, *Kinetics and thermodynamics of cadmium ion removal by adsorption onto nano zerovalent iron particles.* Journal of hazardous materials, 2011. **186**(1): p. 458-465.
82. Contreras Rodríguez, A.R., A. Sánchez Ferrer, and X. Font Segura, Thesis: Removal of cadmium (II), lead (II) and chromium (VI) in water with nanomaterials.Universitat Autònoma de Barcelona 2015.
83. Ayawei, N., A.N. Ebelegi, and D. Wankasi, *Modelling and Interpretation of Adsorption Isotherms.* Journal of Chemistry, 2017. **2017**.
84. Coles, C.A. and R.N. Yong, *Use of equilibrium and initial metal concentrations in determining Freundlich isotherms for soils and sediments.* Engineering Geology, 2006. **85**(1-2): p. 19-25.
85. Li, C., Zhang, L., Xia, H., Peng, J., Zhang, S., Cheng, S. and Shu, J., Kinetics and isotherms studies for congo red adsorption on mesoporous Eupatorium adenophorum-based activated carbon via microwave-induced H3PO4 activation. Journal of Molecular Liquids, 2016. **224**: p. 737-744.
86. Gupta, S.S. and K.G. Bhattacharyya, *Kinetics of adsorption of metal ions on inorganic materials: a review.* Advances in Colloid and Interface Science, 2011. **162**(1-2): p. 39-58.
87. Rahmani, A., H.Z. Mousavi, and M. Fazli, *Effect of nanostructure alumina on adsorption of heavy metals.* Desalination, 2010. **253**(1-3): p. 94-100.
88. Ho, Y.-S., *Review of second-order models for adsorption systems.* Journal of Hazardous Materials, 2006. **136**(3): p. 681-689.
89. El Nemr, A., *Potential of pomegranate husk carbon for Cr(VI) removal from wastewater: Kinetic and isotherm studies.* Journal of Hazardous Materials, 2009. **161**(1): p. 132-141.
90. Bhaumik, M., R. McCrindle, and A. Maity, *Efficient removal of Congo red from aqueous solutions by adsorption onto interconnected polypyrrole–polyaniline nanofibres.* Chemical Engineering Journal, 2013. **228**: p. 506-515.
91. Liu, Y., *New insights into pseudo-second-order kinetic equation for adsorption.* Colloids and Surfaces A: Physicochemical and Engineering Aspects, 2008. **320**(1-3): p. 275-278.
92. Bhaumik, M., Maity, A., Srinivasu, V.V. and Onyango, M.S., Enhanced removal of Cr (VI) from aqueous solution using polypyrrole/$Fe_3O_4$ magnetic nanocomposite. Journal of Hazardous Materials, 2011. **190**(1-3): p. 381-390.
93. Bhaumik, M., Leswifi, T.Y., Maity, A., Srinivasu, V.V. and Onyango, M.S., Removal of fluoride from aqueous solution by polypyrrole/$Fe_3O_4$ magnetic nanocomposite. Journal of Hazardous Materials, 2011. **186**(1): p. 150-159.

94. Setshedi, K.Z., Bhaumik, M., Songwane, S., Onyango, M.S. and Maity, A., Exfoliated polypyrrole-organically modified montmorillonite clay nanocomposite as a potential adsorbent for Cr (VI) removal. Chemical Engineering Journal, 2013. **222**: p. 186-197.
95. Kera, N.H., Bhaumik, M., Pillay, K., Ray, S.S. and Maity, A., Selective removal of toxic Cr (VI) from aqueous solution by adsorption combined with reduction at a magnetic nanocomposite surface. Journal of Colloid and Interface Science, 2017. **503**: p. 214-228.

# CHAPTER 3

# METHODOLOGY

## 3.1 Materials

Pyrrole monomer (Py) (98 %) and anhydrous ferric chloride ($FeCl_3$) were purchased from Sigma–Aldrich (South Africa). Py was distilled under vacuum for purification and stored in the refrigerator until use. Potassium dichromate ($K_2Cr_2O_7$) was obtained from Minema Chemicals (South Africa). Ferrous sulphate heptahydrate ($FeSO_4 \cdot 7H_2O$) was acquired from Glassworld chemicals and suppliers (South Africa). Stock solution (1000 mg/L) of Cr(VI) was prepared by dissolving a pre-determined amount of $K_2Cr_2O_7$ in deionized water. Other chemicals used in this study were of analytical grade. Dried rooibos leaves were purchased from Checkers Hyper (South Africa).

## 3.2 Experimental methods

### 3.2.1 Preparation of Rooibos extract

Rooibos leaves was extracted according to a modified procedure by Diallo *et al.* [1]. Dry leaves (15 g) of rooibos were weighed and transferred into 250 mL of deionized water in a beaker. The mixture was heated for 2 hrs at 80 $^oC$ and a deep orange coloured extract was formed during heating. The solution was left to cool at room temperature. Furthermore, the deep orange extract was filtered and stored in a refrigerator until further use.

### 3.2.2 Synthesis of $Fe^0$ NPs using rooibos extract

Green synthesis method adapted from Wang *et al.* [2] was utilised for the preparation of NPs. For this purpose, rooibos extract was mixed with 0.1 M $FeSO_4 \cdot 7H_2O$ solution and there was an immediate colour change from deep orange to black, indicating the formation of $Fe^0$ NPs. The solution was left to stir overnight. The resulting mixture was centrifuged and washed several times with deionized. Furthermore, it was dried at 60 °C using vacuum oven to obtain the $Fe^0$ NPs.

### 3.2.3 Synthesis of adsorbent

Ppy/$Fe^0$ NC was prepared via *in-situ* chemical oxidative polymerization of Py monomer in the presence of $FeCl_3$ oxidant. During the synthesis process, the amount of $Fe^0$ NPs was varied from 0.1 - 0.2 g with the aim of optimizing the NC for an efficient Cr(VI) sorption. For polymerization, these amounts of $Fe^0$ NPs were added into 80 mL of deionized water in separate 100 mL conical flasks and ultrasonicated for 30 min for better dispersion of the $Fe^0$ NPs. Subsequently, 0.8 mL of Py monomer was syringed to each flask, followed by addition of 0.6 g of $FeCl_3$. The mixture was stirred for 3 hrs at room temperature. The black product formed was then filtered and washed with deionized water until the filtrate became colourless and finally with acetone. The NCs were dried at 60 °C for 8 hrs in a vacuum oven. The total masses of the NC after drying were 1.0602 g, 1.1050 g and 1.1248 g for the $Fe^0$ NPs loading percentages of 18.86 %, 13.57 % and 8.89 %, respectively. The NCs were termed Ppy/$Fe^0$ NC1, Ppy/$Fe^0$ NC2 and Ppy/$Fe^0$ NC3 for 18.86%, 13.57% and 8.89% of $Fe^0$ NPs loading, respectively.

## 3.3 Characterization instruments

### 3.3.1 Ultraviolet-visible (UV-vis) spectroscopy

Absorbance of Cr(VI) solution was carried out using UV-vis spectrophotometer (Perkin Elmar Lambda 750). The samples were analysed in the range 650 - 450 nm. Deionized water was used as a blank reference.

### 3.3.2 Attenuated total reflectance-Fourier transform infrared (ATR-FTIR) spectroscopy

ATR-FTIR spectroscopy analysis of $Fe^0$ NPs, Ppy/$Fe^0$ NC before adsorption and Ppy/$Fe^0$ NC after adsorption was carried out using a Spectrum 100 spectrophotometer (Perkin Elmer, USA) equipped with a germanium crystal and an ATR accessory. The spectra were recorded in the 4000 - 400 $cm^{-1}$ range with the resolution of 4 $cm^{-1}$ and a number of scans per spectrum at 16.

### 3.3.3 X-ray diffraction (XRD) spectroscopy

XRD patterns for the Ppy/$Fe^0$ NC were obtained from a PANalytical X'Pert PRO-diffractometer (PANalytical, The Netherlands), which uses $CuK_\alpha$ radiation ($\lambda$ = 1.5406 Å) at 45 kV/40 mA and $2\theta$ values ranging between 5 and 90˚.

### 3.3.4 Field emission-scanning electron microscopy (FE-SEM)

The surface morphology, structure and elemental composition of the Ppy/$Fe^0$ NC and Ppy homopolymer were investigated using FE-SEM (Auriga Cobra focused-ion beam FIB-SEM). The samples were carbon-coated for SEM analysis and images were obtained using a JEOL-JSM 7500F (USA).

### 3.3.5 High resolution-transmission electron microscopy (HR-TEM)

High-resolution-transmission electron microscope (HR-TEM) was used to investigate the internal morphology of Ppy/$Fe^0$ NC. Samples for HR-TEM were dispersed in ethanol by ultrasonication and dropped onto a carbon coated copper grid. TEM studies were performed on a JEOL-JEM 2100 (Japan) microscope operated at 200 keV.

### 3.3.6 Malvern Zetasizer

The average particle size of the NPs was determined by using Malvern Zetasizer (Nano ZS; Malvern Instrument, Malvern, United Kingdom) at 25 $^oC$. The NPs were filtered using polytetrafluroethylene (PTFE) 0.45 µL pore size membrane and experiment was done in triplicate.

### 3.3.7 Brauner-Emmett-Teller (BET) surface area analysis

BET analysis provides precise specific surface area evaluation of materials by nitrogen multilayer adsorption measured as a function of relative pressure using a fully automated analyzer. The technique includes external area and pore area evaluations to determine the total specific surface area in $m^2/g$ yielding important information in studying the effects of surface porosity and particle size in many applications. BET surface area measurements were obtained from a Micromeritics ASAP 2020 gas adsorption apparatus (Micromeritics, USA) by using the low-temperature $N_2$ adsorption–desorption technique.

### 3.4 Optimization of adsorbent

A comparison of the Cr(VI) removal efficiencies of $Fe^0$, Ppy homopolymer, and Ppy/$Fe^0$ NC was done to determine which adsorbent has the highest removal efficiency. The results indicated that $Fe^0$ NPs, Ppy and Ppy/$Fe^0$ NC had Cr(VI) removal efficiencies of 50.05, 43.14 and 70.4 %, respectively. Ppy/$Fe^0$ NC had higher Cr(VI) removal efficiency as compared to $Fe^0$ NPs and Ppy homopolymer. This might be due to the existence of Ppy polymer matrix around the $Fe^0$ NPs, which increased the mass transfer resistance and then prolonged the time for $Fe^0$ to contact with Cr(VI). Consequently, Ppy/$Fe^0$ NC was chosen as the optimized adsorbent for Cr(VI) removal in the study.

### 3.5 Batch adsorption experiments

Batch adsorption studies were performed to study the effect of adsorption parameters such as adsorbent dose, solution pH, initial Cr(VI) concentration, temperature and co-existing ions on Cr(VI) adsorption by Ppy/$Fe^0$ NC. To evaluate these parameters, different concentrations of Cr(VI) solution were prepared by diluting the $K_2Cr_2O_7$ stock solution (1000 mg/L). For adsorption equilibrium experiments, a fixed amount of Ppy/$Fe^0$ NC (0.025 g) was contacted with 50 mL of Cr(VI) solution in 100 mL plastic bottles in a thermostatic shaker agitated at a speed of 200 rpm for 24 hrs. Thereafter, the samples were filtered using syringe filters and the residual Cr(VI) concentration was measured by the Perkin Elmer Lambda 35 UV–vis spectrometer at 540 nm using 1,5-diphenylcarbazide method. The effects of pH, contact time, adsorbent dose and temperature on Cr(VI) adsorption capacity were explored. The Cr(VI) percentage removal was determined using Eqn. (7):

$$\% \text{ removal} = \frac{C_o - C_e}{C_o} \times 100 \quad (7)$$

Where $C_o$ and $C_e$ are the initial Cr(VI) concentration and the equilibrium Cr(VI) concentration, respectively, in mg/L.

### 3.5.1 Effect of different compositions of the Ppy/$Fe^0$ NC

Assessment of the effect of different compositions of the Ppy/$Fe^0$ NC on removal of Cr(VI) from water was done by contacting 50 mL of 200 mg/L Cr(VI) solution (pH 2) with 0.2 g of Ppy/$Fe^0$ NC1, 015 g of Ppy/$Fe^0$ NC2 and 0.1 g of Ppy/$Fe^0$ NC3 in 100 mL plastic bottles. The bottles were placed in a thermostatic shaker, set at 25 °C and shaken for 24 hrs at 200 rpm. Thus, NC2 which resulted in highest % Cr(VI) removal efficiency was chosen for all the experiments.

### 3.5.2 Effect of pH

The effect of pH on Cr(VI) adsorption by the Ppy/$Fe^0$ NC was studied by varying the solution pH from 2.0 - 12.0. The pH of Cr(VI) solution was adjusted using HCl or NaOH solutions of concentrations 0.01 - 1M.

### 3.5.3 Effect of contact time

In a typical kinetics study, a mixture of Ppy/ $Fe^0$ NC (0.5 g) and Cr(VI) solution (50 mL, pH 2), was stirred in a temperature-controlled water bath at 25 $^oC$. Aliquots (6 mL) were collected at time zero and at selected time intervals, and filtered. For kinetic studies, the capacity of the adsorbent $q_t$ at time t was obtained using Eqn. (8):

$$q_t = \frac{(C_o - C_t)\,V}{m} \quad (8)$$

where $q_t$ (mg/g) is the amount of Cr(VI) adsorbed per unit mass of adsorbent at time t and $c_t$ (mg/L) is the Cr(VI) concentration at time t.

### 3.5.4 Effect of temperature

Adsorption isotherm data was generated by performing experiments at 25, 35 and 45 $^oC$. At a given temperature and pH 2.0, the initial Cr(VI) concentration was varied from 50 to 500 mg/L. The equilibrium sorption capacity was determined using Eqn. (9):

$$q_e = \frac{(C_o - C_e)\,V}{m} \quad (9)$$

where $qe$ is the adsorption capacity of Cr(VI) adsorbed, m is the mass of adsorbent and V is the sample volume (L).

### 3.5.5 Effect of adsorbent dose

The effect of Ppy/$Fe^0$ NC dosage on adsorption of Cr(VI) was examined by varying the mass of adsorbent from 0.025 - 0.1 g. The Cr(VI) initial concentration was 200 mg/L and pH 2.0. The sample volume was 50 mL. The adsorption procedure was similar to that for the effect of pH.

### 3.5.6 Adsorbent regeneration studies

Adsorbent regeneration studies were carried out in order to investigate the potential re-usability of spent Ppy/$Fe^0$ NC. In this study, Cr(VI) was loaded onto Ppy/$Fe^0$ NC by shaking the adsorbent (0.025 g) with Cr(VI) solution (50 mL, 200 mg/L, pH 2) in plastic bottles for 24 hrs. The Cr(VI) loaded Ppy/$Fe^0$ NC was treated with 50 mL of $Na_2CO_3$ solution (0.1 M) by shaking for 24 hrs to desorb the Cr(VI) from the adsorbent. The adsorbent was regenerated after desorption by shaking with 2 M HCl for 4 hrs. Three treatment cycles were carried out in order to study the potential of re-using Ppy/$Fe^0$ NC for Cr(VI) removal from aqueous solution. All the adsorption, desorption and regeneration steps were performed in a temperature controlled shaker set at 25 °C.

### 3.5.7 Effect of co-existing ions

The effect of co-existing ions ($Cu^{2+}$, $Zn^{2+}$, $Co^{2+}$, $Ni^{2+}$, $Cl^-$, $NO_3^-$, $PO_4^{2-}$ and $SO_4^{2-}$) were selected at different concentrations in solutions on Cr(VI) adsorption by Ppy/$Fe^0$ NC. In a typical experiment, 50 mL of 200 mg/L Cr(VI) solutions containing the ion of interest was contacted with of Ppy/$Fe^0$ NC (0.025 g) by shaking for 24 hrs in a thermostatic shaker at 25 °C. The concentration of the co-existing ions in the Cr(VI) solution was varied from 50 - 200 mg/L. After equilibrium was reached the solutions were filtered and the Cr(VI) concentration of the solutions determined as previously described.

## REFERENCES


1. Diallo, A., Beye, A.C., Doyle, T.B., Park, E. and Maaza, M., Green synthesis of Co3O4 nanoparticles via Aspalathus linearis: physical properties. Green Chemistry Letters and Reviews, 2015. **8**(3-4): p. 30-36.
2. Wang, T., Lin, J., Chen, Z., Megharaj, M. and Naidu, R., Green synthesized iron nanoparticles by green tea and eucalyptus leaves extracts used for removal of nitrate in aqueous solution. Journal of cleaner production, 2014. **83**: p. 413-419.

# CHAPTER 4

# RESULTS AND DISCUSSION

## SECTION 1: Characterization of $Fe^0$ NPs, Ppy and Ppy/$Fe^0$ NC

### 4.1 ATR-FTIR

The ATR-FTIR spectra of $Fe^0$ NPs, Ppy/$Fe^0$ NC before and Ppy/$Fe^0$ NC after adsorption are shown in Figure 4.1. The spectra displayed a stretching vibration at 1600 $cm^{-1}$ for the -C=C, 1000 $cm^{-1}$ for C-O-C absorption peak. A broad peak in the range of 3000 - 3500 $cm^{-1}$ appeared in the spectra of $Fe^0$ NPs and the Ppy/$Fe^0$ NC after adsorption which corresponds to the -O-H of the polyphenols. Moreover, the broad peak in the Ppy/$Fe^0$ NC after adsorption had its intensity decreased due to the Ppy polymer matrix. Peak shifting were observed in the Ppy/$Fe^0$ NC after adsorption as compared to the Ppy/$Fe^0$ NC before adsorption. This clearly showed that a chemical reaction has taken place. Interestingly, a small peak at 1500 $cm^{-1}$ in the Ppy/$Fe^0$ NC before adsorption disappeared in the Ppy/$Fe^0$ NC after adsorption. Another peak at around 500 $cm^{-1}$ appeared in the Ppy/$Fe^0$ NC after adsorption which is not present in the Ppy/$Fe^0$ NC before adsorption. Peaks observed between 850 - 1000 $cm^{-1}$ in the $Fe^0$ NPs spectrum corresponds to –C=H and $–CH_2$ bending of the aromatic groups present in the plant extract, which are being adsorbed by the NPs in the form of polyphenols during its synthesis. All these groups present in the surface of NPs act as stabilizing agents after its synthesis.

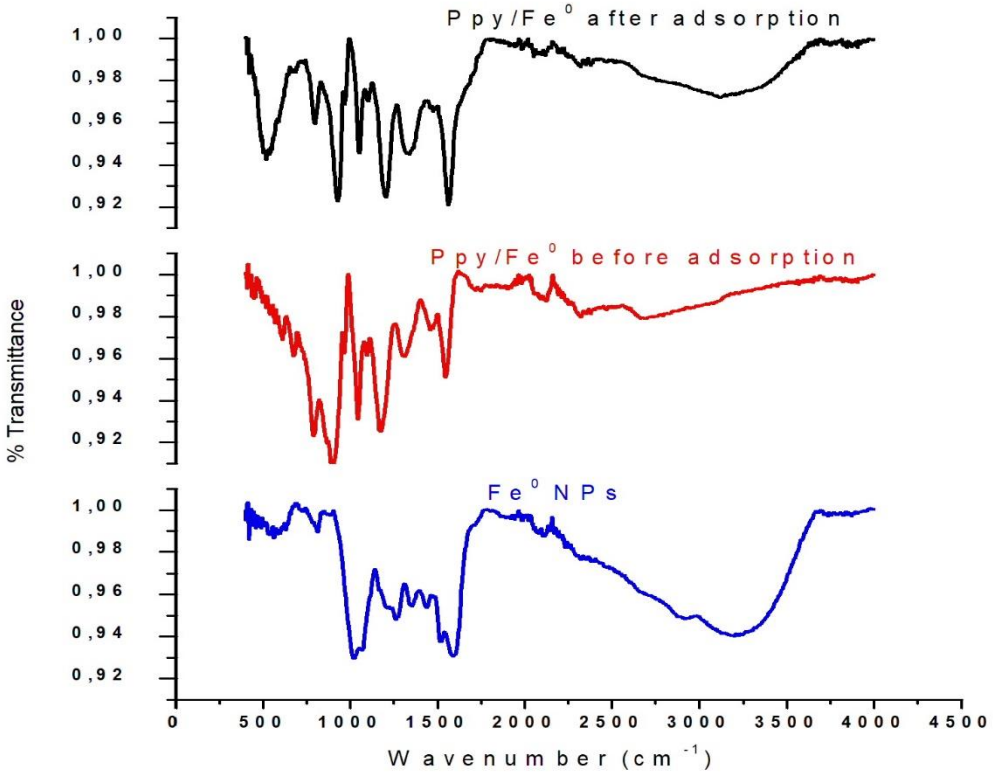


**Figure 4. 1:** ATR-FTIR spectra of $Fe^0$ NPs, Ppy/$Fe^0$ NC before and after adsorption.

### 4.2 X-ray diffraction

The XRD was used to confirm the incorporation of $Fe^0$ NPs in the Ppy matrix upon the synthesis of the NC before and after adsorption and the results are shown in Figure 4.1. A broad peak at approximately 2θ = 25° was observed in Ppy/$Fe^0$ NC before adsorption, which is a characteristic peak of amorphous Ppy matrix [1] and a strong peak at 2θ = 44.8° corresponding to the 110 plane for crystalline $Fe^0$ NPs [2]. It is interesting to notice that the peak at 2θ = 25° in the Ppy/$Fe^0$ NC after adsorption has disappeared. This may be due to the adsorption of Cr(VI). Additionally, the broad shoulder peaks at 2θ = 10° in the spectra of Ppy/$Fe^0$ NC before and after adsorption was proposed to be as a result of the presence of organic materials like polyphenols and flavanoids from leaf extract which are responsible for capping/stabilizing the $Fe^0$ NPs [3].

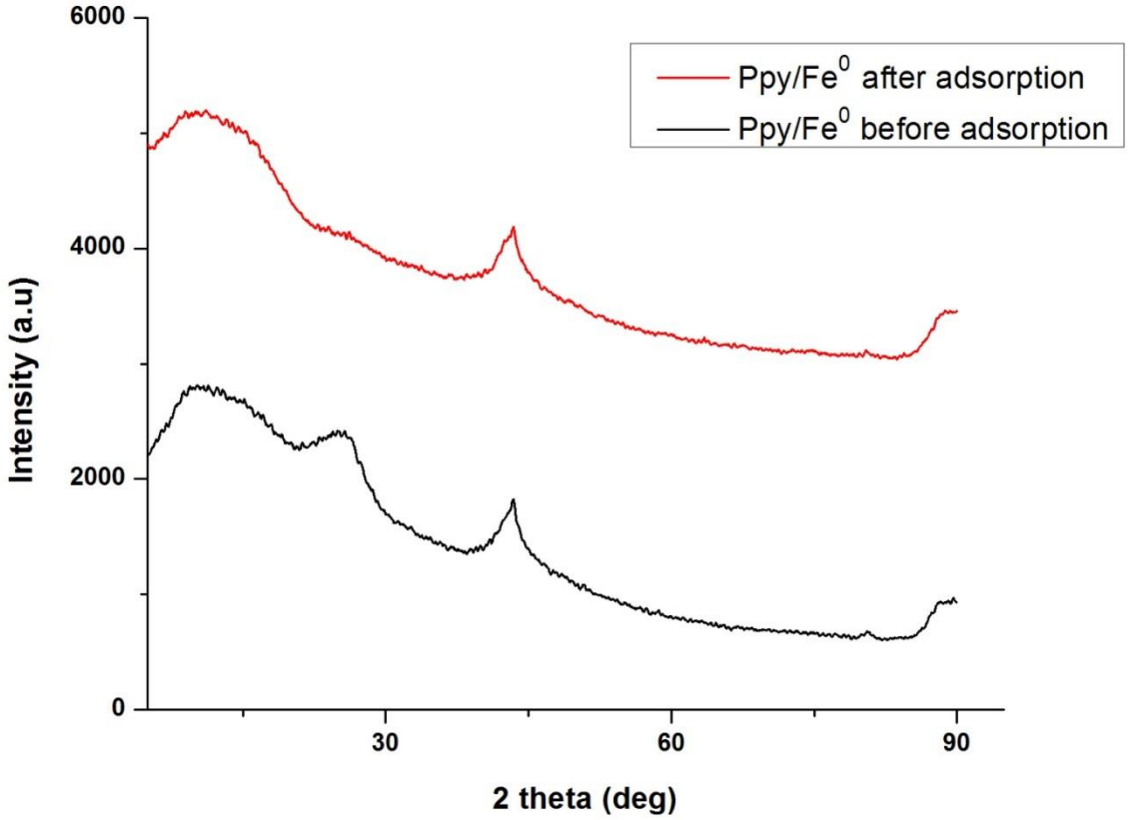


**Figure 4. 2:** *XRD patterns of Ppy/Fe$^0$ NC before and after adsorption.*

### 4.3 SEM analysis

Figure 4.2 presents the surface morphology of the Ppy and Ppy/Fe$^0$ NC obtained using FE-SEM. The Ppy image shows that the Ppy homopolymer consists of highly agglomerated spherically shaped particles (see Figure 2(a)), which is similar to previous studies by Ballav *et al*. [4] and Bhaumik *et al*. [5]. Upon NC formation, it is noticeable that the particle size was reduced as is shown in Figure 4.3(b). After an *in-situ* polymerization process, an agglomeration of smaller sizes were observed in Ppy/Fe$^0$ NC. Moreover, the NC displayed some interstices between particles which could influence the increase in metal adsorption. These findings are similar to a study done by Kera *et al*. [6] where Ppy was modified with *m*-phenylenediamine (mPD). The surface morphology of the nanocomposite after polymerization did not change.

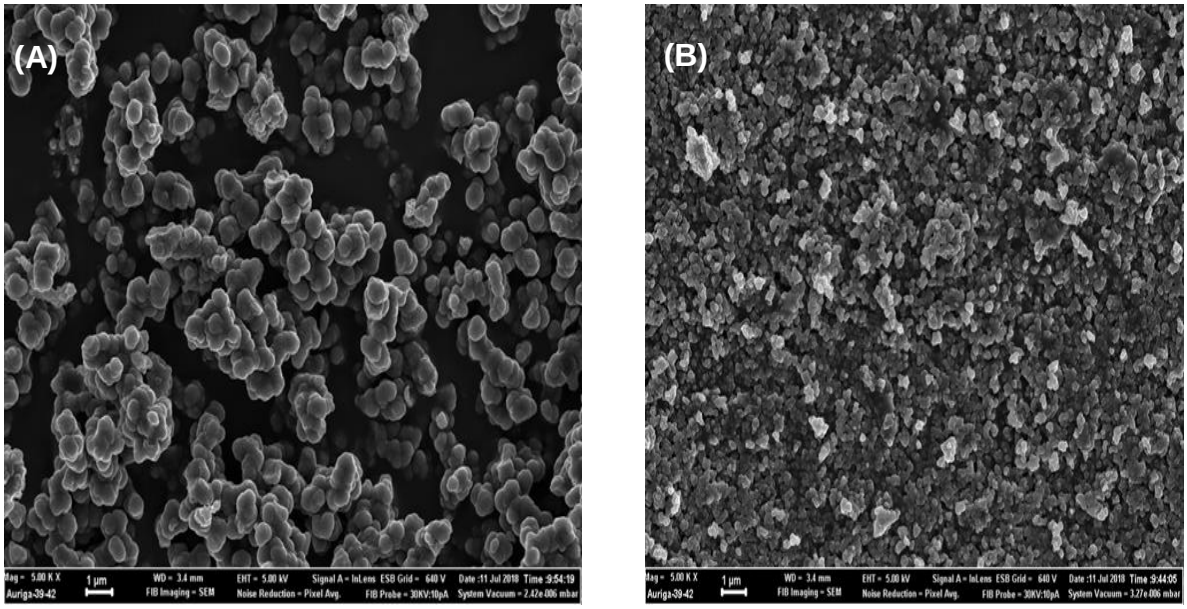


**Figure 4. 3:** SEM images of a) Ppy homopolymer and b) Ppy/$Fe^0$ NC.

### 4.4 EDX

The energy dispersive X-ray (EDX) was utilized to confirm the adsorption of Cr(VI) ions by Ppy/$Fe^0$ NC before and after adsorption as depicted in Figure 4.4. For Ppy/$Fe^0$ NC before adsorption, the spectrum showed peaks due to C, O and Cl appearing at 0.3, 0.5 and 2.62 keV, respectively. It is interesting to note that after adsorption of Cr(VI), the nanocomposites showed two additional peaks at 5.4 and 5.8 KeV for Cr. These peaks suggest successful adsorption of Cr(VI) ions onto the Ppy/$Fe^0$ NC.

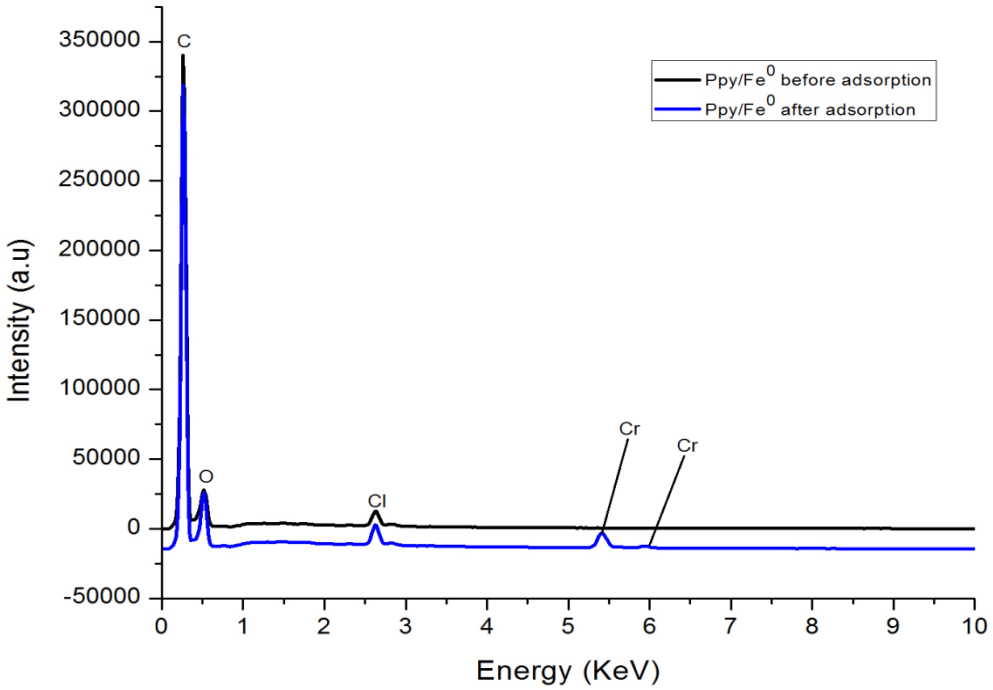


**Figure 4. 4:** EDX of Ppy/$Fe^0$ NC before and after Cr(VI) adsorption.

### 4.5 TEM analysis

The HR-TEM was used to examine the structure of the prepared Ppy/$Fe^0$ NC, as depicted in Figure 4.5 (a) and (b). The figure shows that $Fe^0$ NPs are distributed across the Ppy polymer matrix. The darker core is $Fe^0$ NPs and light coloured shell is amorphous Ppy polymer. TEM image shows a composite layered structure comprising of a dense metallic centre enclosed by a thin layer. Similar findings were reported by Bhaumik *et al*. [7] describing that the $Fe_3O_4$ NPs were embedded in the Ppy matrix for the Ppy/$Fe_3O_4$ NC.

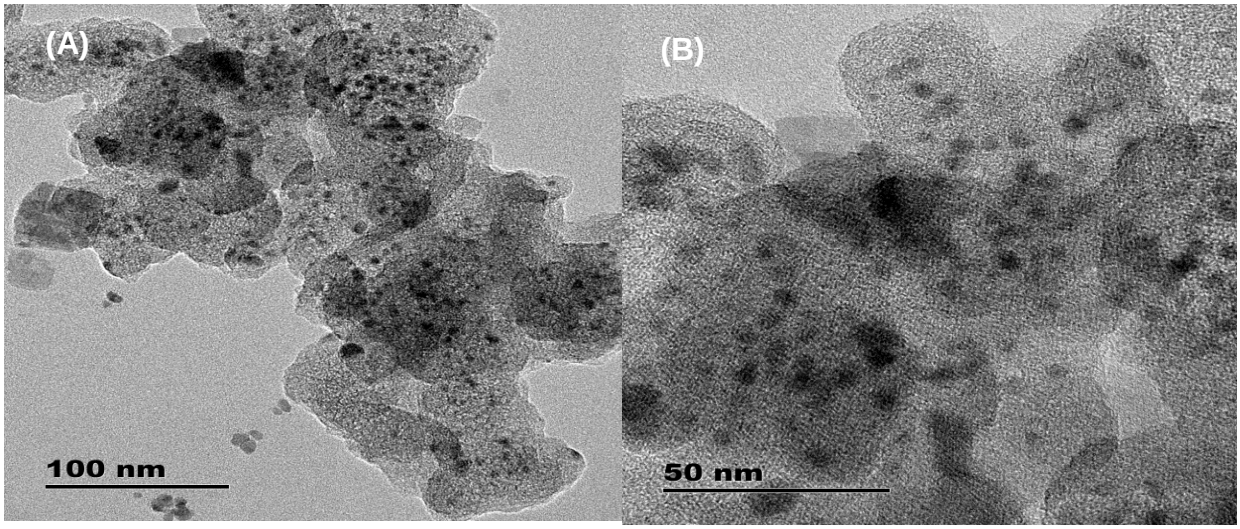


**Figure 4. 5:** HR-TEM images of Ppy/$Fe^0$ NC.

### 4.6 Particle size of $Fe^0$ NPs

Malvern Zetasizer was used to measure the particle size of the synthesized NPs. Figure 4.6 shows the size distribution of the NPs. The NPs have a mean size of 121.9 nm. The obtained results indicated that the $Fe^0$ NPs are entirely within the nanoscale range. These results are similar to a study by the Katata-Seru *et al*.[8] were Moringa oleifera leaves (MOL) and Moringa oleifera seeds (MOS) were used to synthesize FeNPs for nitrate removal from water. The particle size found was in the range 138-474 nm.

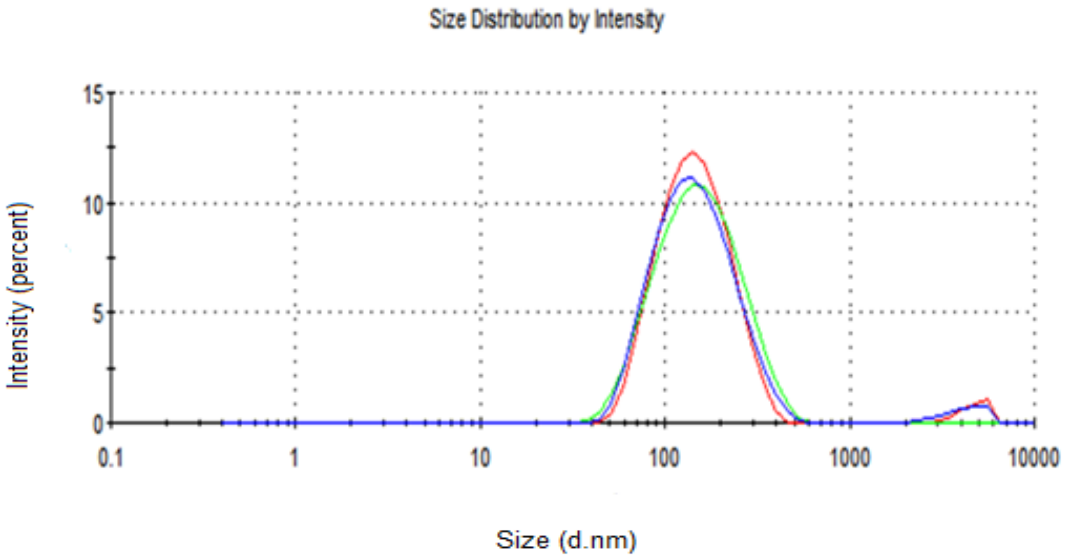


**Figure 4. 6:** Particle size distribution of $Fe^0$ NPs.

### 4.7 BET

The surface area of the Ppy/$Fe^0$ NC was measured from the BET method using the $N_2$ adsorption-desorption curves. The BET specific surface area, average pore volume and average pore diameter, were found to be 45.13 $m^2/g$, 14.72 $cm^3/g$ and 0.12 nm, respectively. In comparison, Kera *et al*. [6] found BET specific surface area, average pore diameter, and average pore volume of 5.0 $m^2/g$, 49.45 nm and 0.01 $cm^3/g$ respectively, for Ppy. Therefore, these results show that the incorporation of $Fe^0$ into Ppy resulted in a significant increase in the BET surface area and average pore volume, and a corresponding decrease in the average pore diameter. The increase in BET surface area corresponds well to the smaller particle size observed from the SEM image of Ppy/$Fe^0$ NC.

## SECTION 2: Evaluation of the Ppy/$Fe^0$ NC on Cr(VI) adsorption

### 4.8 Effect of pH

The pH of a solution is one of the most important parameters that governs metal adsorption on an adsorbent, due to its controlling effect on the nature of the physico-chemical interaction of the species in the solution and the adsorption sites of the adsorbents [5]. The effect of initial solution pH on Cr(VI) removal efficiency by Ppy/$Fe^0$ NC is shown in Figure 4.6. The pH studies were carried out between 2.0 - 12.0, the adsorption of Cr(VI) by Ppy/$Fe^0$ NC largely depends on the pH of the solution. As the pH of the solution was increased, the Cr(VI) removal decreased (73 - 32%). A reduction in the removal efficiency at higher pH values may be due to the deprotonation of the nitrogen atoms of the Ppy matrix and competitive interaction between Cr(VI) anions and hydroxyl ions molecules present in the reaction solution [9]. The high removal observed at low pH is probably due to reduction of Cr(VI) to Cr(III) [10].

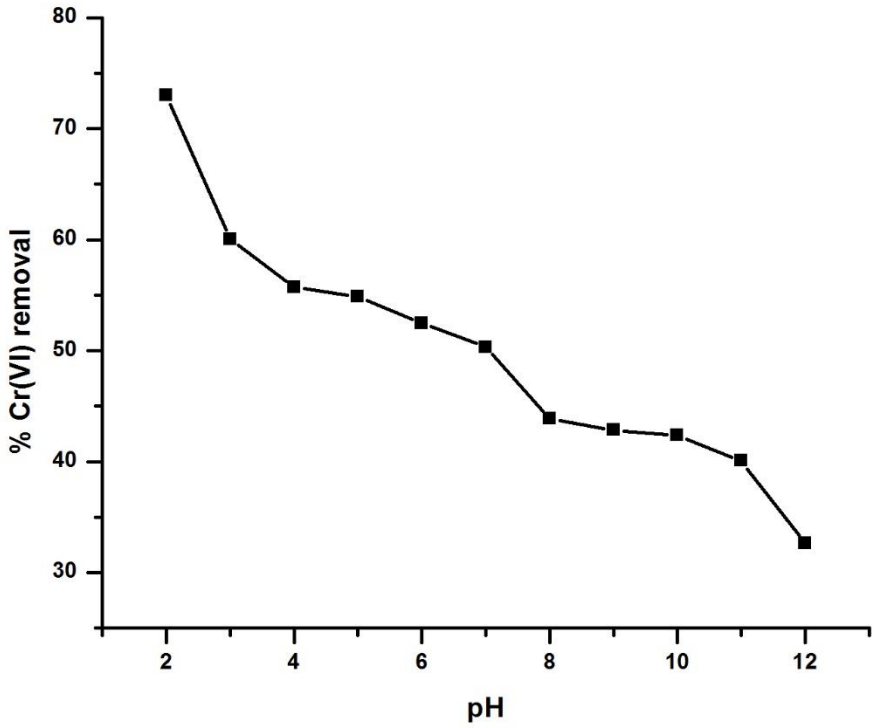


**Figure 4.7:** Effect of pH on Cr(VI) removal using Ppy/$Fe^0$ NC.

Furthermore, the maximum Cr(VI) adsorption by Ppy/$Fe^0$ NC was achieved at pH 2.0. At pH 2 – 6, the most prevailing Cr(VI) species in solution are the $HCrO_4^-$ and $Cr_2O_7^{2-}$ oxyanions, which become $CrO_4^{2-}$ as the pH increases above 6 as seen in Figure 4.7 [11].

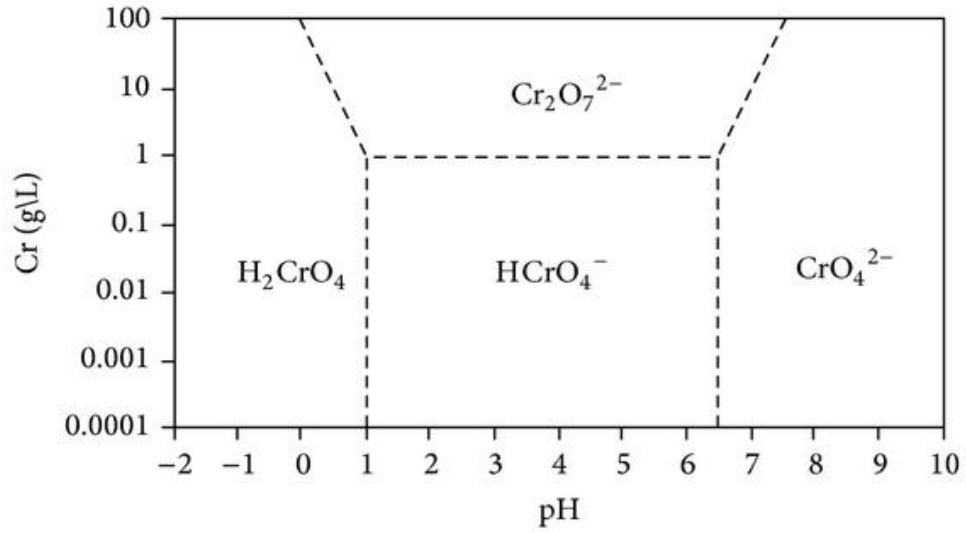


**Figure 4.8:** Cr(VI) speciation in an aqueous environment as a function of Cr(VI) concentration and pH [12].

### 4.9 Effect of adsorbent dose

The effect of adsorbent dose was performed in order to determine the minimum amount of Ppy/$Fe^0$ NC required to remove all the Cr(VI) from the solution at pH 2.0 (200 mg/L, 50 mL) and the results are depicted in Figure 4.8. The removal efficiency increased from 60.78% - 98.81% with an increase in Ppy/$Fe^0$ NC dose from 0.01 - 0.1 g as a result of accessibility of more adsorption sites for Cr(VI). As the Ppy/$Fe^0$ NC dose was increased from 0.05 g - 0.1 g, the removal efficiency remained constant as the Cr(VI) in solution was the limiting factor. An adsorbent dose of 0.05 g per 50 mL of 200 mg/L Cr(VI) solution was therefore the optimum adsorbent mass required for complete removal of Cr(VI) from solution. In a similar study to investigate the effect of adsorbent dose on Cr(VI) removal, Kera *et al*. [1] used Ppy/DABSA and found that 0.05 g of Ppy/DABSA composite for the treatment of 50 mL of a 100 mg/L Cr(VI) solution was required for 100% removal of Cr(VI) from aqueous solution. At lower adsorbent concentration number of active sites in Ppy$Fe^0$ NC is higher. With

increasing the adsorbent dosage, there is formation of aggregate of particles, which has a greater influence on the Cr(VI) uptake [13].

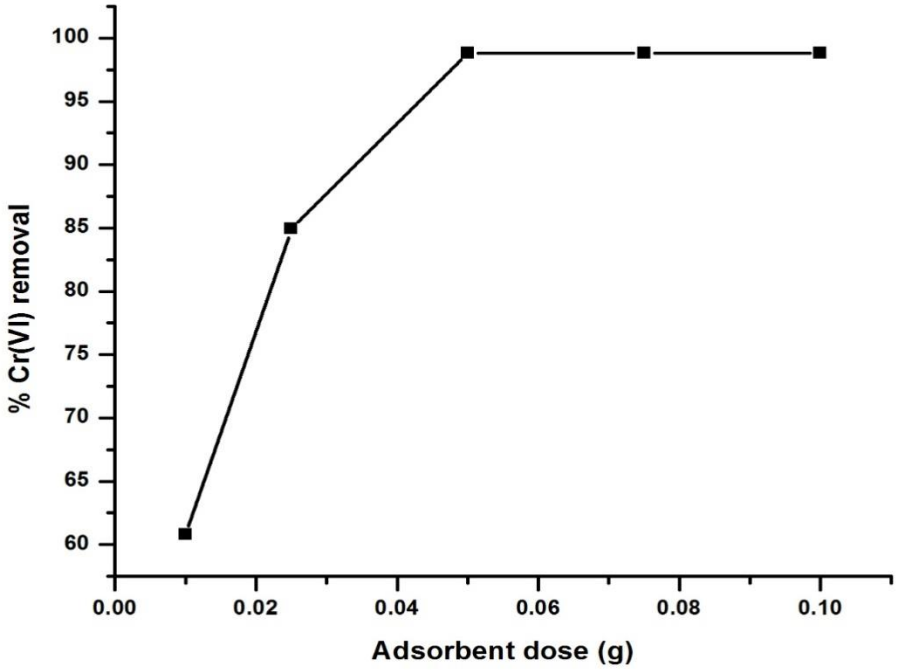


**Figure 4.9:** Effect of adsorbent dose on Cr(VI) removal by Ppy/$Fe^0$ NC.

### 4.10 Adsorption isotherm

Adsorption isotherms provide a crucial information about interaction between the adsorbent and adsorbate, as well as to evaluate the maximum capacity of the adsorbent [14]. The isotherm studies were performed at pH 2 and various temperatures of 15, 25, and 45℃ for the removal of Cr(VI) using Ppy/$Fe^0$ NC and the results are presented in Figure 4.9. It can be seen that the adsorption capacity increased with increasing the temperature. This may result from an increase in thermal energy of the adsorbing species which leads to higher adsorption capacity [15]. The Cr(VI) adsorption capacity increased with temperature suggesting the endothermic nature of the adsorption process.

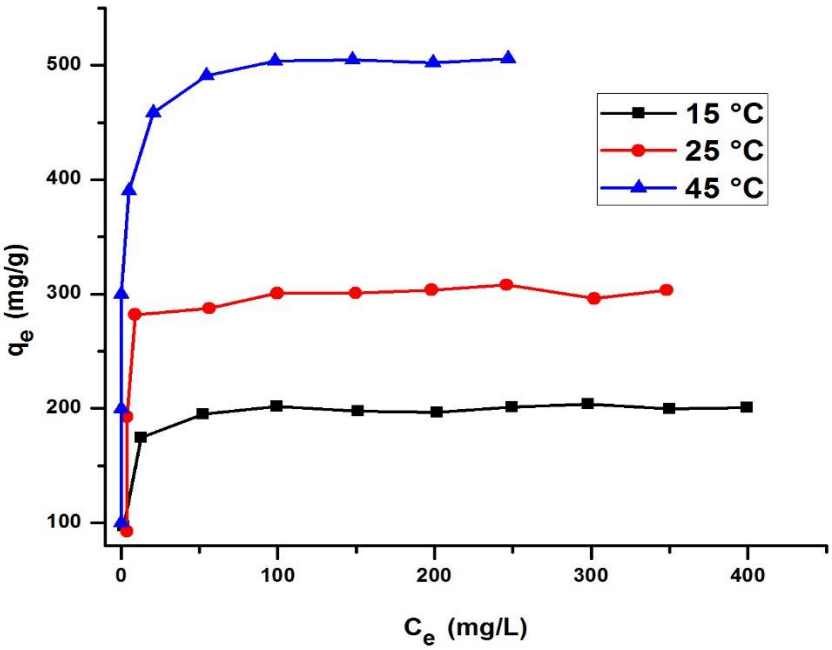


**Figure 4.10:** Effect of temperature on Cr(VI) removal by Ppy/$Fe^0$ NC.

In this study, the adsorption data were fitted into two commonly used isotherm models, namely, Langmuir and Freundlich models. The non-linear forms of Langmuir and Freundlich models are presented in Eqs (10) and (11), respectively [16].

$$\frac{q_e}{q_m} = \frac{bC_e}{1+bC_e} \tag{10}$$

$$q_e = K_f C_e^{1/n} \tag{11}$$

where $q_m$ (mg/g) is the Langmuir maximum adsorption capacity, $K_F$ (mg/g) is the Freundlich constant related to the adsorption capacity, *b* (L/mg) is the Langmuir constant related to the energy of adsorption, and 1/n is the Freundlich constant related to the intensity of adsorption. Eqs (12) and (13) present the linear forms of Langmuir and Freundlich models, respectively [17]:

$$\frac{C_e}{q_e} = \frac{C_e}{q_m} + \frac{1}{K_L q_m} \tag{12}$$

$$\ln q_e = \ln K_f \frac{1}{n} \log C_e \tag{13}$$

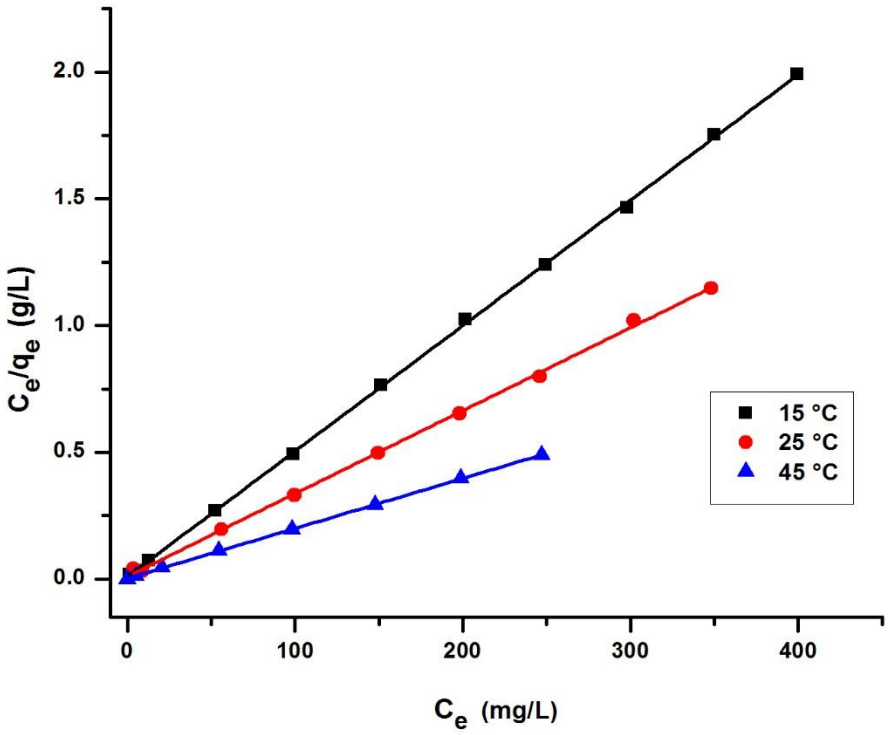


**Figure 4.11:** Fit of data to linearized Langmuir isotherm model.

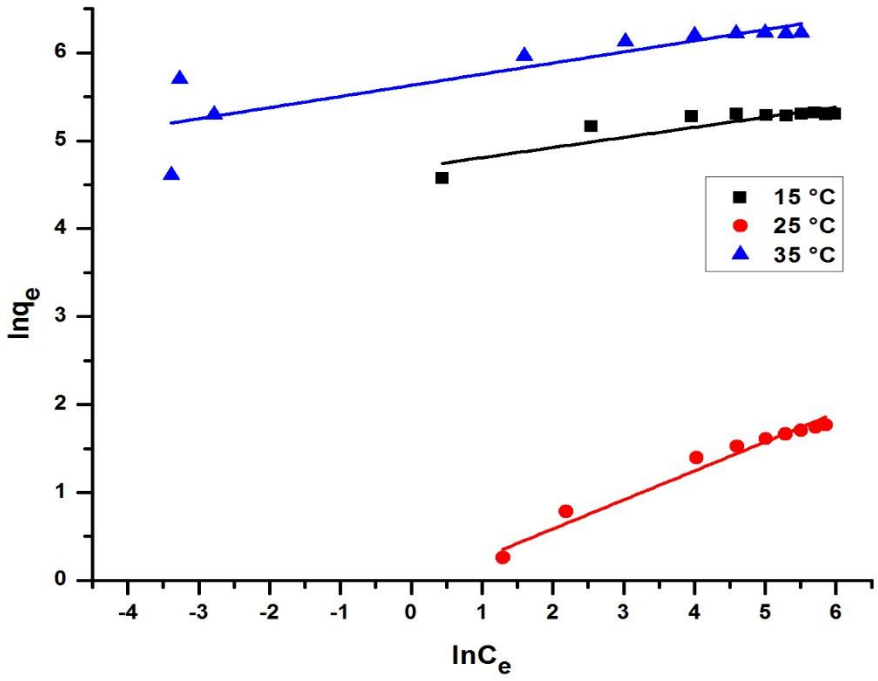


**Figure 4.12:** Fit of data to linearized Freundlich isotherm model.

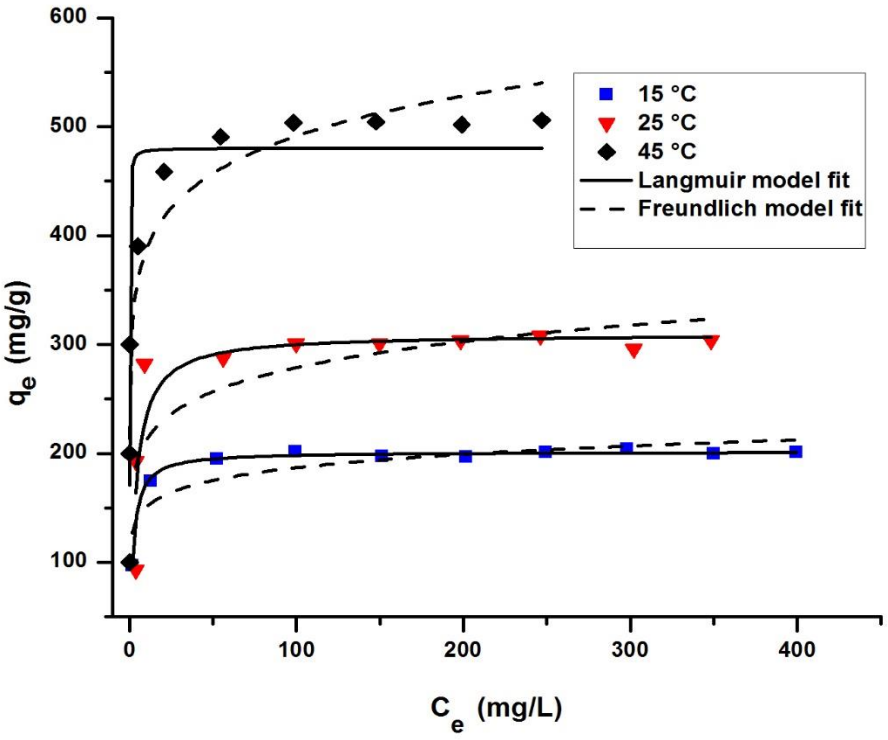


**Figure 4.13:** Fit of data to Langmuir and Freundlich isotherm kinetic model.

The isotherm data obtained was further analysed by using both Langmuir and Freundlich models (linear and non-linear) which are illustrated in Figures 4.10 – 4.12. Table 4.1 presents the parameters calculated by fitting the data to the Langmuir and Freundlich isotherm models. From the correlation coefficient ($R^2$) values obtained, it is noticeable to observe that the Langmuir isotherm model gave a better description of adsorption data in this study, with higher $R^2$ values for the linear and non-linear fitting. A higher value of n ($n > 1$) indicates favourable adsorption, whereas $n < 1$ represents poor adsorption characteristics [18]. These results also suggest that Cr(VI) adsorption occurs by the formation of a monolayer in a finite number of identical adsorption sites on a homogeneous surface.

**Table 4. 1:** Isotherm parameters for Cr(VI) adsorption by Ppy/$Fe^0$ NC

| **Isotherm model** | **Temperature** | | |
|---|---|---|---|
| | **15 °C** | **25 °C** | **45 °C** |
| **Langmuir** | | | |
| ***Linear*** | | | |
| $q_m$ | 202.02 | 305.8 | 505.05 |
| *b* | 0.54 | 0.33 | 1.17 |
| $R^2$ | 0.99974 | 0.99915 | 0.99991 |
| ***Non-linear*** | | | |
| Best-fit values | | | |
| $q_m$ | 201.6 | 309.7 | 480.6 |
| *b* | 0.579 | 0.3059 | 16.26 |
| Std. Error | | | |
| *qm* | 0.8691 | 13.85 | 23.33 |
| *b* | 0.0271 | 0.09332 | 5.222 |
| 95% Confidence Intervals | | | |
| $q_m$ | 199.6 - 203.6 | 277.7 - 341.6 | 426.8 - 534.4 |
| *b* | 0.5165 - 0.6415 | 0.09071 - 0.5211 | 4.213 - 28.30 |
| Goodness of Fit | | | |
| Degrees of Freedom | 8 | 8 | 8 |
| $R^2$ | 0.9952 | 0.7927 | 0.8458 |
| Absolute Sum of Squares | 46.1 | 9130 | 30071 |
| Sy.x | 2.401 | 33.78 | 61.31 |
| Number of points Analyzed | 10 | 10 | 10 |
| **Freundlich** | | | |
| ***Linear*** | | | |
| $K_F$ | 109.185 | 0.928 | 278.8 |
| *n* | 8.686 | 3.031 | 7.88 |
| $R^2$ | 0.76742 | 0.97372 | 0.72378 |
| ***Non-linear*** | | | |
| Best-fit values | | | |
| $K_F$ | 121.8 | 161 | 303.9 |
| *n* | 10.77 | 8.388 | 9.578 |
| Std. Error | | | |
| $K_F$ | 12.92 | 29.57 | 25.21 |
| *n* | 2.419 | 2.649 | 1.693 |
| 95% Confidence Intervals | | | |
| $K_F$ | 92.03 - 151.6 | 92.85 - 229.2 | 245.8 - 362.0 |
| *n* | 5.195 - 16.35 | 2.281 - 14.50 | 5.675 - 13.48 |
| Goodness of Fit | | | |

| | | | |
|---|---|---|---|
| Degrees of Freedom | 8 | 8 | 8 |
| $R^2$ | 0.773 | 0.6221 | 0.8651 |
| Absolute Sum of Squares | 2178 | 16646 | 26295 |
| Sy.x | 16.5 | 45.62 | 57.33 |
| Number of points Analyzed | 10 | 10 | 10 |

Units: $q_m$ = maximum adsorption capacity (mg/g), $n$ = adsorption intensity,$K_F$ = adsorption capacity (mg/g), $b$ = Langmuir constant (L/mg).

The adsorption capacity of Ppy/$Fe^0$ NC was compared with other adsorbents reported in literature [5, 19-23] in Table 4.2. It can be observed that the adsorption capacity of the Ppy/$Fe^0$ NC is relatively higher than other adsorbents. The results shows that PpyFe$^0$ NC is therefore a promising adsorbent for the removal of Cr(VI) from aqueous solutions due to its high adsorption capacity and relatively easy and low-cost synthesis.

**Table 4. 2 :** Comparison of the Cr(VI) adsorption capacity of Ppy/$Fe^0$ NC with other adsorbents

| **Adsorbent** | $q_m$ **(mg/g)** | **Optimum pH** | **Reference** |
|---|---|---|---|
| Ppy/OMWCNTs | 294 | 2 | [5] |
| Ppy-OMMT | 119.34 | 2 | [19] |
| Ppy-PANI | 227 | 2 | [20] |
| Ppy-$Fe_3O_4$/rGO | 293.3 | 3 | [21] |
| Ppy/$Fe_3O_4$ | 208.77 | 2 | [22] |
| PAN/Ppy | 61.80 | 2 | [23] |
| Ppy/$Fe^0$ NC | 305.8 | 2 | Present work |

### 4.11 Adsorption kinetics

The effect of contact time on Cr(VI) adsorption is depicted in Figure 4.13. At low initial concentration, the adsorption capacity increased quickly with an increase in the concentration of Cr(VI). However, there was a delay in tendency of increase at high initial concentration. The reason could be that most of the adsorption sites had been occupied and it was difficult for Cr(VI) anions to enter the vacant sites for adsorption [24]. The figure shows that Cr(VI) adsorption capacity increased with an increase in

contact time and with an increase in initial concentration. For the initial Cr(VI) concentration of 25 mg/L, equilibrium was reached within 75 min. The time required to reach equilibrium increased with an increase in initial concentration from 50 - 100 mg/L.

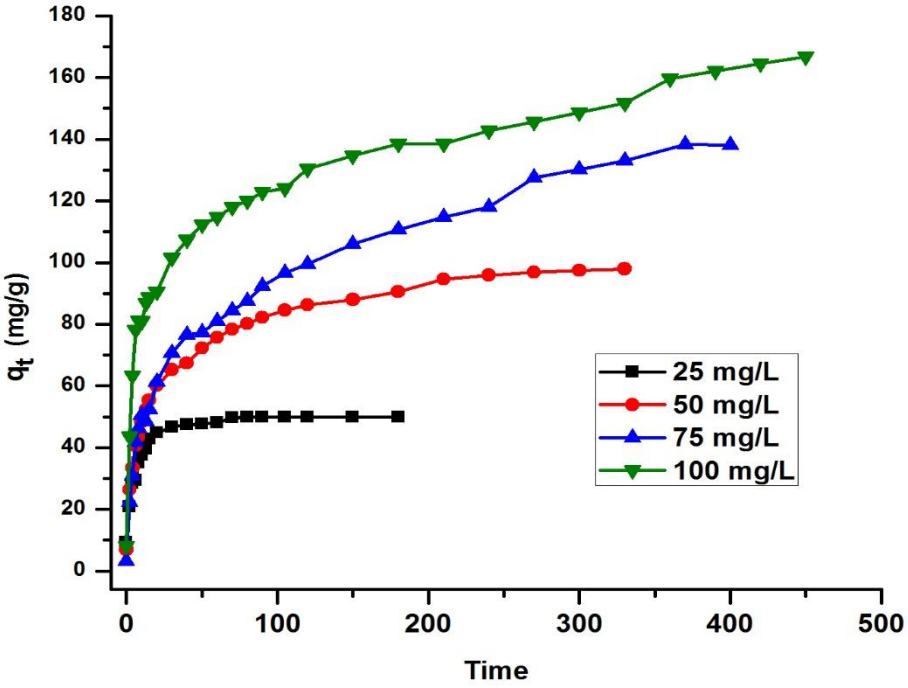


**Figure 4.14:** Effect of contact time on Cr(VI) removal by Ppy/$Fe^0$ NC.

In order to investigate the adsorption kinetics further, the pseudo-first-order and pseudo-second-order kinetic model were applied to evaluate the adsorption process of Cr(VI). Figure 4.14 and 4.15 shows the linear fit of the pseudo-first-order and pseudo-second-order kinetics, while Figure 4.16 represents the non-linear pseudo-first order and pseudo-second order.The linear forms of the pseudo-first-order and pseudo-second-order kinetic model areas shown by Eqs. (14) and (15), respectively [25]:

$$q_{t=} q_e (1-e^{-k1t}) \quad (14)$$

$$q_t = \frac{k_2 q_e^2 t}{1 + k_2 q_e t} \quad (15)$$

where *qe* (mg/g) and *qt* (mg/g) are the adsorption capacities at equilibrium and time t (min) and $k_1$ (1/min) and $k_2$ (g/mg/min) are the pseudo-first-order and pseudo-

second-order rate constants, respectively. Eqs. (16) and (17), respectively represents the linear forms of the pseudo-first order and pseudo-second order kinetic models [26]:

$$\log (q_e - q_t) = \log q_e - \frac{K_1}{2.303} t \quad (16)$$

$$\frac{t}{qt} = \frac{1}{K_2 q_e^2} + \frac{t}{q_e} \quad (17)$$

From pseudo second kinetic model, the initial sorption rate, $h_0$ (mg/g/min) can be defined as [27]:

$$h_0 = k_2 q_e^2 \ (t \rightarrow 0) \quad (18)$$

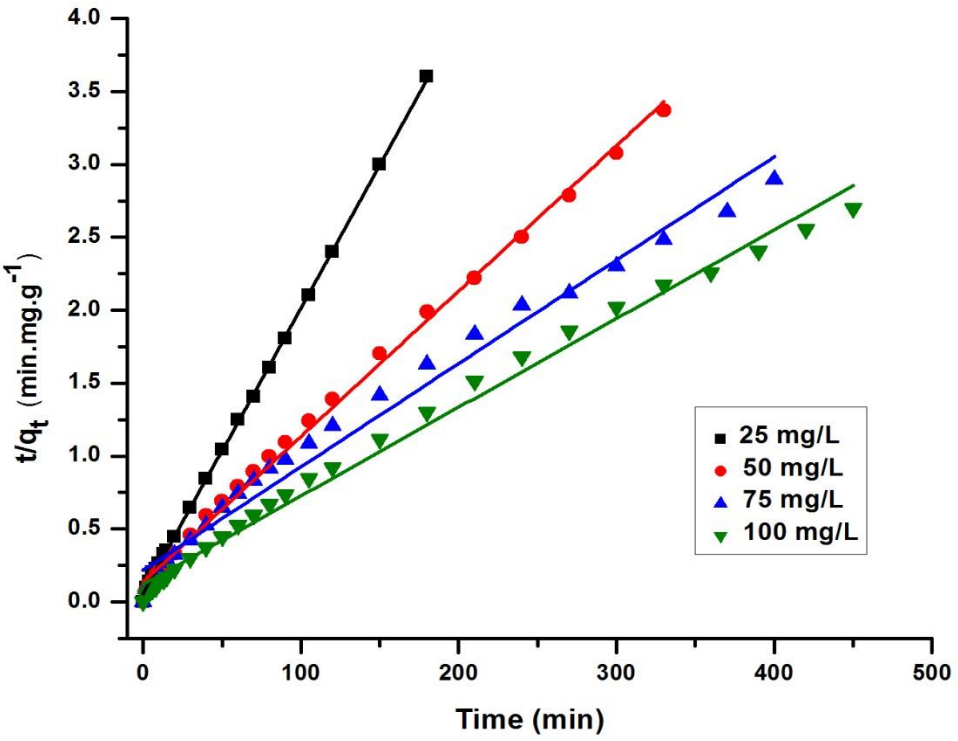


**Figure 4.15:** Fit of data to linearized pseudo-second order kinetic model.

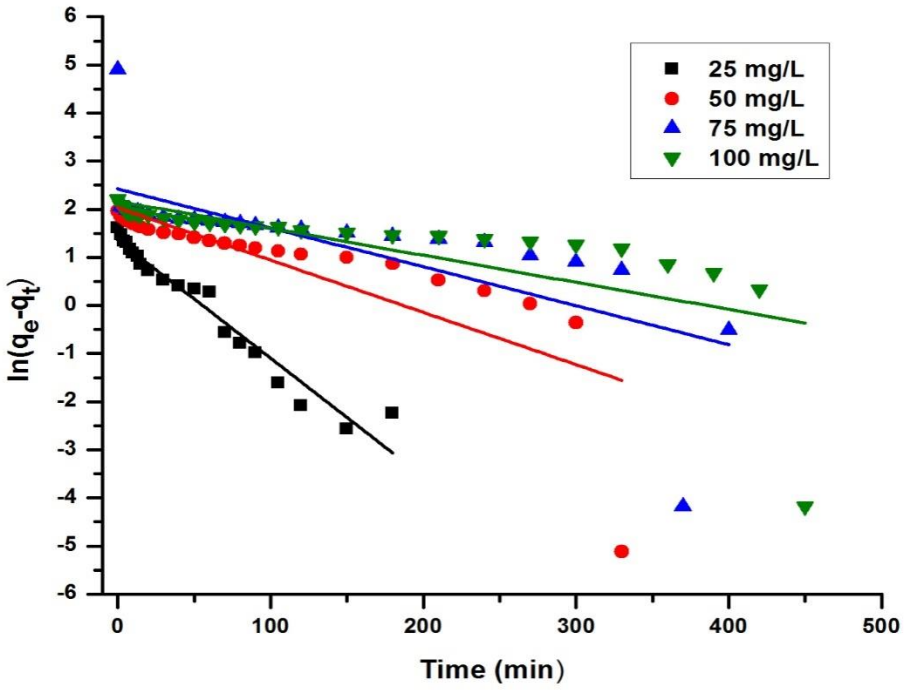


**Figure 4.16:** Fit of data to linearized pseudo-second order kinetic model.

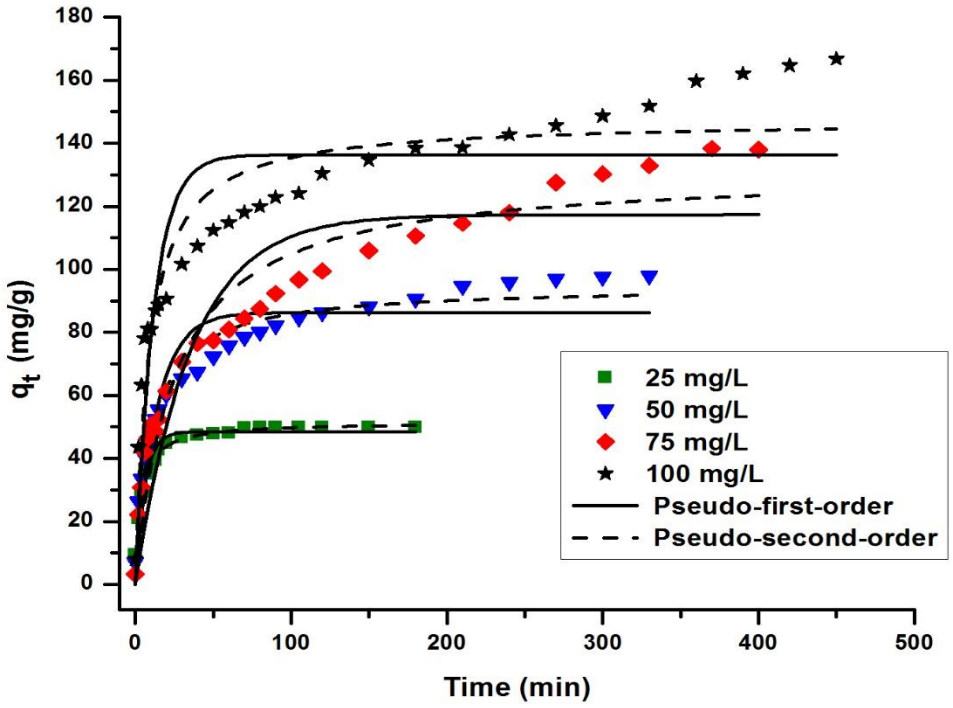


**Figure 4.17:** Fit of data to pseudo-first-order and pseudo-second-order kinetic models.

It can be observed from Table 4.2 that the high values of the correlation coefficients ($R^2$), for the linear and non-linear pseudo-second-order model gave better description of the Cr(VI) adsorption by Ppy/$Fe^0$ NC compared to pseudo-first-order model. The data fitted the pseudo-second order better that the pseudo-first order.

**Table 4.3:** Kinetic parameters for Cr(VI) adsorption by Ppy/$Fe^0$ NC

| **Kinetic model** | **Initial Cr(VI) concentration** | | | |
|---|---|---|---|---|
| | **25 ppm** | **50 ppm** | **75 ppm** | **100 ppm** |
| **Pseudo first order** | | | | |
| ***Linear*** | | | | |
| $q_e$ | 3.89 | 7.599 | 11.309 | 8.733 |
| $k_1$ | 0.0565 | 0.249 | 0.019 | 0.0129 |
| $R^2$ | 0.95092 | 0.61549 | 0.50183 | 0.47881 |
| ***Non-linear*** | | | | |
| Best-fit values | | | | |
| $q_e$ | 48.47 | 86.28 | 117.3 | 136.3 |
| $k_1$ | 0.1703 | 0.07318 | 0.0282 | 0.08586 |
| Std. Error | | | | |
| *qe* | 0.9721 | 2.377 | 4.722 | 4.223 |
| $k_1$ | 0.01679 | 0.009164 | 0.004395 | 0.01371 |
| 95% Confidence Intervals | | | | |
| $q_e$ | 46.43 - 50.51 | 81.36 - 91.20 | 107.6 - 127.1 | 127.6 - 145.0 |
| $k_1$ | 0.1350 - 0.2056 | 0.05422 - 0.09214 | 0.01915 - 0.03726 | 0.05773 - 0.1140 |
| Goodness of Fit | | | | |
| Degrees of Freedom | 18 | 23 | 25 | 27 |
| $R^2$ | 0.9192 | 0.8798 | 0.845 | 0.7803 |
| Absolute Sum of Squares | 201.5 | 1803 | 5669 | 8932 |
| Sy.x | 3.346 | 8.854 | 15.06 | 18.19 |
| Number of points Analyzed | 20 | 25 | 27 | 29 |
| **Pseudo second order** | | | | |
| ***Linear*** | | | | |
| $q_e$ | 51.05 | 100.3 | 141.04 | 164.47 |
| $K_2$ | 0.00672 | 0.000725 | 0.000232 | 0.000311 |
| $h_0$ | 17.51 | 7.29 | 4.62 | 8.41 |
| $R^2$ | 0.99965 | 0.99674 | 0.98322 | 0.99157 |
| ***Non-linear*** | | | | |

| | | | | |
|---|---|---|---|---|
| Best-fit values | | | | |
| $q_e$ | 0.005495 | 0.001033 | 0.0003045 | 0.0007723 |
| $k_2$ | 51.5 | 94.62 | 131.1 | 147.3 |
| Std. Error | | | | |
| $q_e$ | 0.0006722 | 0.00012 | 0.00005365 | 0.0001287 |
| $k_2$ | 0.8997 | 1.866 | 4.551 | 3.675 |
| 95% Confidence Intervals | | | | |
| $q_e$ | 0.004082 - 0.006907 | 0.0007846 - 0.001281 | 0.0001939 - 0.0004150 | 0.0005081 - 0.001036 |
| $k_2$ | 49.61 - 53.39 | 90.76 - 98.48 | 121.7 - 140.5 | 139.8 - 154.9 |
| Goodness of Fit | | | | |
| Degrees of Freedom | 18 | 23 | 25 | 27 |
| $R^2$ | 0.9568 | 0.9593 | 0.9281 | 0.8968 |
| Absolute Sum of Squares | 107.8 | 610.8 | 2628 | 4196 |
| Sy.x | 2.447 | 5.154 | 10.25 | 12.47 |
| Number of points Analyzed | 20 | 25 | 27 | 29 |

Units: $q_e$: mg/g, $k_1$: 1/min, $k_2$: g/mg.min, $h_0$: mg/g/min.

### 4.12 Adsorbent regeneration studies

Regeneration studies help with the recovery of the adsorbent from wastewater and the reusing of the adsorbent. Regeneration ability of adsorbents is an essential factor for the development of cost effective removal process. The Ppy/$Fe^0$ NC after Cr(VI) adsorption was treated with 50 mL of $Na_2CO_3$ solution (0.1 M) by shaking for 24 hrs to desorb the Cr(VI) from the NC. Regeneration studies were carried out by shaking NC with 2M HCl (50 mL) for 4 hrs. Three treatment cycles were carried out in order to study the reusability of Ppy/$Fe^0$ NC for Cr(VI) removal from aqueous solution. It can be seen in Figure 4.17 that the removal efficiency for the cycle was 65%, however, the removal efficiency was reduced to 34% and 26% in the second and third cycles, respectively. The decrease in adsorption capacity may be due to the deterioration of the polymer chain by repeated oxidation reaction with highly oxidizing Cr(VI) species, thereby reducing the sorption sites available for the used adsorbent [20]. These results suggests that the Ppy/$Fe^0$ NC can be reused successfully for the removal of Cr (VI) for one cycle without loss of its removal efficiency.

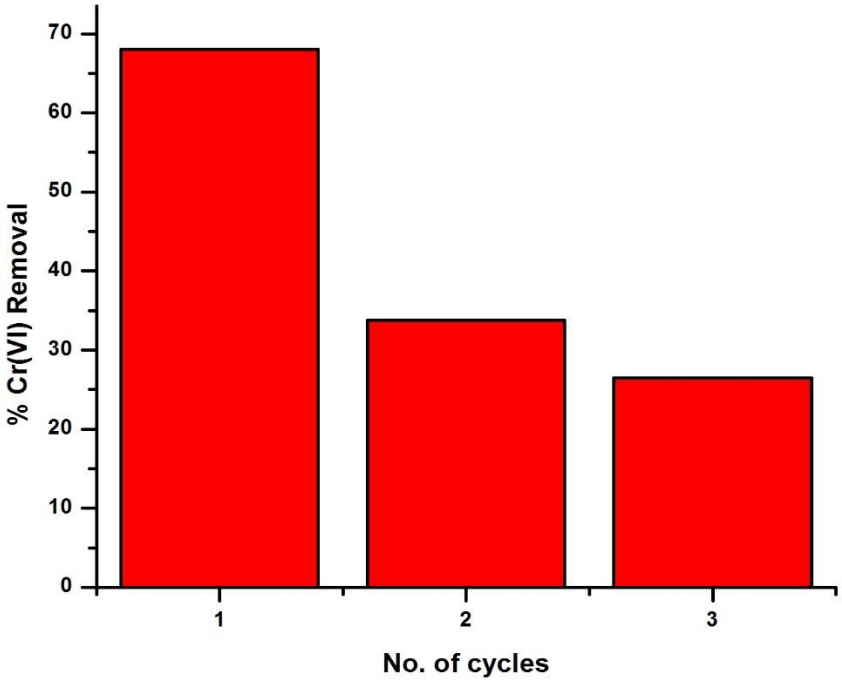


**Figure 4.18:** Adsorption cycles for Cr(VI) removal by Ppy/$Fe^0$ NC.

### 4.13 Effect of co-existing ions

Mining, electroplating and other industries produce wastewater that contains high levels of Cr(VI) as well as other dissolved anions and cations [28-30]. Therefore, it is essential to investigate the competition between co-existing ions and Cr(VI) in solution for adsorption sites by Ppy/$Fe^0$ NC. The effect of selected ions ($Ni^{2+}$, $Cu^{2+}$, $Zn^{2+}$, $Co^{2+}$, $NO_3^-$, $Cl^-$, $PO_4^{2-}$ and $SO_4^{2-}$) on Cr(VI) removal by the synthesized NC was studied by varying the co-existing ions concentrations in solution from 50 – 200 mg/L, with the Cr(VI) at 200 mg/L and the results are presented in Figure 4.18. The results revealed that both anions and cations in solution at varying concentrations do not have a significant effect on the removal of Cr(VI) by Ppy/$Fe^0$ NC. At low pH, cations in solution are repelled from the positively charged surface of the NC, and therefore, do not affect Cr(VI) removal. It was expected that anions such as $Cl^-$, $NO_3^-$, $PO_4^{2-}$ and $SO_4^{2-}$ would compete with Cr(VI) because they are negatively charged. One possible reason is that $Cl^-$, $NO_3^-$, $PO_4^{2-}$ and $SO_4^{2-}$ are weaker oxidizing agents than $HCrO_4^-$, i.e. they are not reduced by Ppy/$Fe^0$ NC and therefore

do not affect Cr(VI) adsorption [31]. Thus, it can be concluded that the removal of Cr(VI) by Ppy/$Fe^0$ is selective in nature.

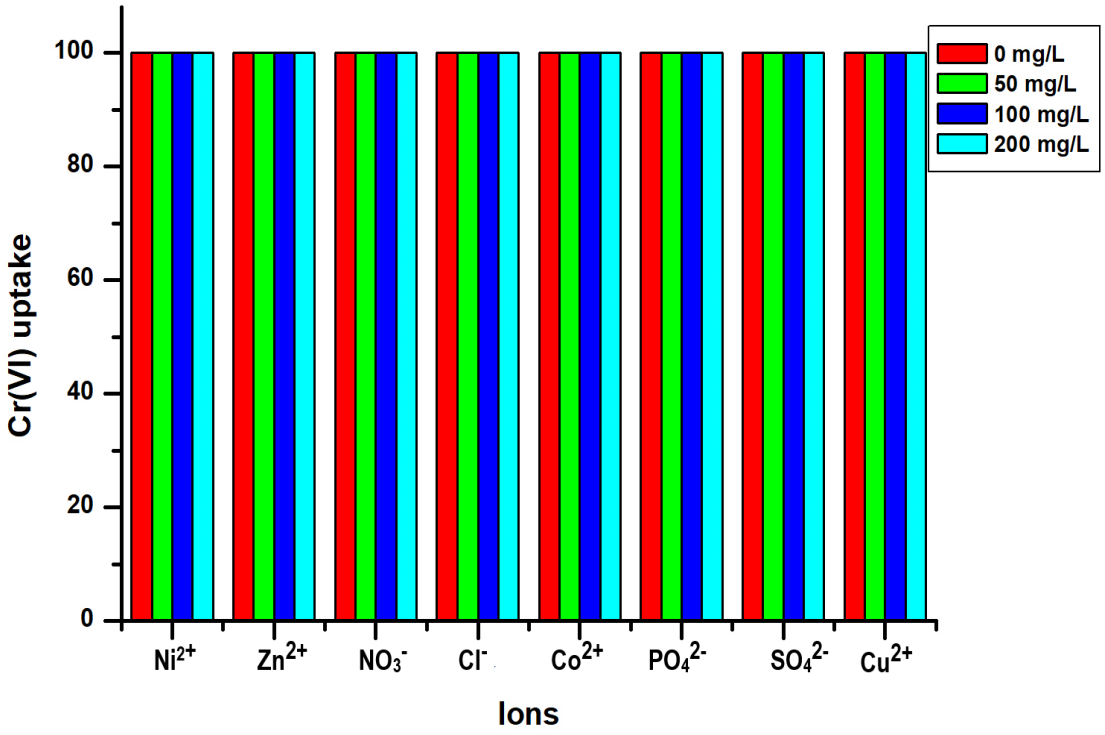


**Figure 4.19:** The effect of co-existing ions on Cr(VI) adsorption by Ppy/$Fe^0$ NC

## REFERENCES


1. Kera, N.H., Bhaumik, M., Ballav, N., Pillay, K., Ray, S.S. and Maity, A., Selective removal of Cr(VI) from aqueous solution by polypyrrole/2,5-diaminobenzene sulfonic acid composite. Journal of Colloid and Interface Science, 2016. **476**: p. 144-157.
2. Zhu, B.-W., T.-T. Lim, and J. Feng, *Reductive dechlorination of 1, 2, 4-trichlorobenzene with palladized nanoscale Fe0 particles supported on chitosan and silica.* Chemosphere, 2006. **65**(7): p. 1137-1145.
3. Soliemanzadeh, A., Fekri, M., Bakhtiary, S. and Mehrizi, M.H., Biosynthesis of iron nanoparticles and their application in removing phosphorus from aqueous solutions. Chemistry and Ecology, 2016. **32**(3): p. 286-300.
4. Ballav, N., A. Maity, and S.B. Mishra, *High efficient removal of chromium(VI) using glycine doped polypyrrole adsorbent from aqueous solution.* Chemical Engineering Journal, 2012. **198**: p. 536-546.
5. Bhaumik, M., Agarwal, S., Gupta, V.K. and Maity, A., Enhanced removal of Cr (VI) from aqueous solutions using polypyrrole wrapped oxidized MWCNTs nanocomposites adsorbent. Journal of Colloid and Interface Science, 2016. **470**: p. 257-267.
6. Kera, N.H., Bhaumik, M., Pillay, K., Ray, S.S. and Maity, A., m-Phenylenediamine-modified polypyrrole as an efficient adsorbent for removal of highly toxic hexavalent chromium in water. Materials Today Communications, 2018. **15**: p. 153-164.
7. Bhaumik, M., R. McCrindle, and A. Maity, Efficient removal of Congo red from aqueous solutions by adsorption onto interconnected polypyrrole–polyaniline nanofibres. Chemical Engineering Journal, 2013. **228**: p. 506-515.
8. Katata-Seru, L., Moremedi, T., Aremu, O.S. and Bahadur, I., *Green synthesis of iron nanoparticles using Moringa oleifera extracts and their applications: Removal of nitrate from water and antibacterial activity against Escherichia coli.* Journal of Molecular Liquids, 2018. **256**: p. 296-304.
9. Bhaumik, M., R. McCrindle, and A. Maity, *Efficient removal of Congo red from aqueous solutions by adsorption onto interconnected polypyrrole–polyaniline nanofibres.* Chemical Engineering Journal, 2013. **228**: p. 506-515.
10. Anah, L.; Astrini, N. Influence of pH on Cr(VI) ions removalfrom aqueous solutions using carboxymethyl cellulose-based hydrogel as adsorbent. IOP Conference Series Earth and Environmental Sciences 2017, **60**, p.012010.
11. Tan, Y.Y., Wei, C., Gong, Y.Y. and Du, L.L., Adsorption of hexavalent chromium onto sisal pulp/polypyrrole composites. IOP Conference Series: Materials Science and Engineering. 2017. **170**(1): p. 012007.
12. Du Preez, S., Thesis: *Cr(VI) generation during flaring of off-gas from closed ferrochromium submerged arc furnaces.*North West University. 2014.
13. Padmavathy, K., G. Madhu, and P. Haseena, *A study on effects of pH, adsorbent dosage, time, initial concentration and adsorption isotherm study for the removal of hexavalent chromium (Cr (VI)) from wastewater by magnetite nanoparticles.* Procedia Technology, 2016. **24**: p. 585-594.
14. Wang, J., K. Zhang, and L. Zhao, *Sono-assisted synthesis of nanostructured polyaniline for adsorption of aqueous Cr (VI): effect of protonic acids.* Chemical Engineering Journal, 2014. **239**: p. 123-131.

15. Bhaumik, M., Maity, A., Srinivasu, V.V. and Onyango, M.S., Enhanced removal of Cr(VI) from aqueous solution using polypyrrole/$Fe_3O_4$ magnetic nanocomposite. Journal of Hazardous Materials, 2011. **190**(1): p. 381-390.
16. Bhaumik, M., V.K. Gupta, and A. Maity, *Synergetic enhancement of Cr(VI) removal from aqueous solutions using polyaniline@Ni(OH)$_2$ nanocomposites adsorbent.* Journal of Environmental Chemical Engineering, 2018. **6**(2): p. 2514-2527.
17. Inyinbor, A., F. Adekola, and G. Olatunji, *Kinetics, isotherms and thermodynamic modeling of liquid phase adsorption of Rhodamine B dye onto Raphia hookerie fruit epicarp.* Water Resources and Industry, 2016. **15**: p. 14-27.
18. Panda, H., Tiadi, N., Mohanty, M. and Mohanty, C.R., Studies on adsorption behavior of an industrial waste for removal of chromium from aqueous solution. south african Journal of Chemical Engineering, 2017. **23**: p. 132-138.
19. Setshedi, K.Z., Bhaumik, M., Songwane, S., Onyango, M.S. and Maity, A., Exfoliated polypyrrole-organically modified montmorillonite clay nanocomposite as a potential adsorbent for Cr(VI) removal. Chemical Engineering Journal, 2013. **222**: p. 186-197.
20. Bhaumik, M., Maity, A., Srinivasu, V.V. and Onyango, M.S., Removal of hexavalent chromium from aqueous solution using polypyrrole-polyaniline nanofibers. Chemical Engineering Journal, 2012. **181**: p. 323-333.
21. Wang, H., Yuan, X., Wu, Y., Chen, X., Leng, L., Wang, H., Li, H. and Zeng, G., Facile synthesis of polypyrrole decorated reduced graphene oxide–$Fe_3O_4$ magnetic composites and its application for the Cr(VI) removal. Chemical Engineering Journal, 2015. **262**: p. 597-606.
22. Aigbe, U.O., Das, R., Ho, W.H., Srinivasu, V. and Maity, A., A novel method for removal of Cr(VI) using polypyrrole magnetic nanocomposite in the presence of unsteady magnetic fields. Separation and Purification Technology, 2018. **194**: p. 377-387.
23. Wang, J., Pan, K., He, Q. and Cao, B., *Polyacrylonitrile/polypyrrole core/shell nanofiber mat for the removal of hexavalent chromium from aqueous solution.* Journal of hazardous materials, 2013. **244**: p. 121-129.
24. Liu, X., Y. Liao, and H. Gao, *Enhancement adsorption of hexavalent chromium from aqueous solution on polypyrrole using ethylamine group.* Journal of Dispersion Science and Technology, 2017: p. 1-9.
25. Moussout, H., Ahlafi, H., Aazza, M. and Maghat, H., Critical of linear and nonlinear equations of pseudo-first order and pseudo-second order kinetic models. Karbala International Journal of Modern Science, 2018.
26. Chigondo, M., Paumo, H.K., Bhaumik, M., Pillay, K. and Maity, A., Rapid high adsorption performance of hydrous cerium-magnesium oxides for removal of fluoride from water. Journal of Molecular Liquids, 2018. **265**: p.496-509.
27. Bhaumik, M., Maity, A., Srinivasu, V.V. and Onyango, M.S., Enhanced removal of Cr(VI) from aqueous solution using polypyrrole/$Fe_3O_4$ magnetic nanocomposite. Journal of Hazardous Materials, 2011. **190**(1-3): p. 381-390.
28. Chauke, V.P., A. Maity, and A. Chetty, *High-performance towards removal of toxic hexavalent chromium from aqueous solution using graphene oxide-alpha cyclodextrin-polypyrrole nanocomposites.* Journal of molecular liquids, 2015. **211**: p. 71-77.
29. Hamilton, E.M., Young, S.D., Bailey, E.H. and Watts, M.J., Chromium speciation in foodstuffs: a review. Food Chemistry, 2018. **250**: p. 105-112.

30. Burbridge, D.J., Koch, I., Zhang, J. and Reimer, K.J., Chromium speciation in river sediment pore water contaminated by tannery effluent. Chemosphere, 2012. **89**(7): p. 838-843.
31. Liu, W., Yang, L., Xu, S., Chen, Y., Liu, B., Li, Z. and Jiang, C., Efficient removal of hexavalent chromium from water by an adsorption–reduction mechanism with sandwiched nanocomposites. Royal Society of Chemistry Advances, 2018. **8**(27): p. 15087-15093.

# CHAPTER 5

# CONCLUSION AND RECOMMENDATIONS

## 5.1 Conclusion

In this study, green synthesized $Fe^0$ NPs encapsulated in Ppy polymer, Ppy/$Fe^0$ NCs, was successfully prepared by the *in-situ* chemical oxidative polymerization method for the removal of Cr(VI) from aqueous solution. The removal efficiency of the NC was evaluated on Cr(VI) removal from aqueous solution at laboratory scale. Different parameters like effect of pH, adsorbent dose, temperature, time and co-existing ions were studied to investigate the removal of Cr(VI) by Ppy/$Fe^0$ NC.

SEM images showed that Ppy homopolymer and Ppy/$Fe^0$ NC consists of spherical and aggregated particles.The core/shell structure of the NC can be clearly seen from the TEM images. The specific surface area of the synthesized NC was found to be 80.53 $m^2.g^{-1}$ by the BET method. EDX confirmed the attachment of Cr(VI) ions onto the Ppy/$Fe^0$ NCs after adsorption. Additionally, the XRD confirmed the incorporation of $Fe^0$ NPs in the Ppy polymer matrix and peak shifting were observed in the Ppy/$Fe^0$ NC after adsorption as compared to the Ppy/$Fe^0$ NC before adsorption in the FTIR spectra.

The initial solution's pH had a noticeable effect on the Cr(VI) removal, which increased as the pH decreased. The Cr(VI) removal efficiency increased with an increase in Ppy/$Fe^0$ NC dose. The adsorption data fitted the pseudo-second-order model and Langmuir isotherm model. The Ppy/$Fe^0$ NC is highly selective and could only be used for one cycle. Therefore, further studies are required to study the potential of the NC for removal of Cr(VI) from industrial wastewater. Based on the findings from the study, it is believed that results obtained may assist the wastewater treatment field with easy and safe removal of heavy metals from water. These findings suggest that Ppy/$Fe^0$ NC has potential to be used in Cr(VI) removal from water.

## 5.2 Recommendations

The following recommendations were drawn from results and suggested as follow up to this study:

1. Though the NC showed satisfactory results in the removal of Cr(VI) from aqueous solutions, the results showed that the NC can be used for only one cycle. Hence there is a need to study the encapsulation of $Fe^0$ NPs onto other polymers.
2. Perform experiments below pH 2.
3. Characterize using thermal gravimetric analysis (TGA) to study the thermal stability of the NC.
4. Study the thermodynamic parameters and mechanical properties of NC.
5. Use IC-ICP-MS to study the speciation of Cr(VI) at different solution pH.